Ref. no. : 86-007
File no. : 8724-12433
Date : January 1986
P

Title

EVALUATION OF TWO MATHEMATICAL WIND TURBINE WAKE MODELS IN VARIOUS TYPES OF FLOW

Author(s):
E. Luken
A.M. Talmon
P.E.J. Vermeulen

Keyword(s):
- wind energy
- wind turbine wake effects

Carried out within the Dutch Development Programme for Wind Energy (NOW) 2, fase 1; financed by the Ministry of Economic affairs.

Job 8.8.3
IEA - 9 - NL 03

CONTENTS page

NOMENCLATURE

b	wake width	[m]
C_D (= - C_T)	drag coefficient (= $D/\frac{1}{2}\rho U_{ref}^2.\pi R^3$)	-
C_p	power coefficient (= $P/\frac{1}{2}\rho U_{ref}^3\ \pi R^2$)	-
C_T	thrust coefficient (= $T/\frac{1}{2}\rho U_{ref}^2\ \pi R^2$)	-
D	drag	[kg m/s^2]
D	rotor diameter	[m]
k	turbulent energy $\frac{1}{2}(u_i'\ u_i')$	[m^2/s^2]
k_1, k_2, k_3	turbulent interaction constants	
L_u, L_v, L_w	length scale of turbulence in u, v, w direction	[m]
m	centerline velocity deficit decay rate constant	-
m	axial induction factor (= $(1-C_t)^{-1}$)	-
n	MILLY calculation factor (= $\frac{X_{NW}}{X_H}$)	-
P	Power	[kg.m^2/s^3]
R	rotor radius (= D/2) (also used as wake radius) in fig. 10	[m]
T	thrust	[kg m/s^2]
U	time averaged air speed	[m/s]
U_d	velocity deficit (= $1-\frac{U}{U_{ref}}$)	[m/s]
u', v', w'	turbulent velocity fluxtuation in 1, y and z direction respectively	[m/s^2]
x, y, z	cartesian coordinates, x in direction of undisturbed wind speed	
α	"characteristic" ambient turbulence in MILLY programme ($\sqrt{u'^2}$; $\sqrt{v'^2}$; $\sqrt{w'^2}$)	[m/s]
$\sigma_{u,v,w}$	turbulence intensity	
ε	turbulent eddy viscosity	[m^2/s]
ρ	air density	[kg/m^3]

INDEX

a	ambient value
cl	centerline value
m	shear induced
ref	reference value (in wind tunnel meas. outside the wake)
w	within wake
α	due to ambient turbulence
λ	rotor induced
∞	undisturbed situation

SUMMARY

In order to investigate the effects of tower and nacelle, as well as those of turbulent shear flow on the wind-turbine wake, wind tunnel experiments on a 0.36 m diameter horizontal-axis wind-turbine model have been carried out. These experiments consist of two series of measurements. The first series has been performed in low turbulent ($\sigma_u \sim 0.56\%$) uniform flow over a fixed ground plane using a lattice and a circular shaped tower and two nacelle configurations (circular and rectangular respectively).
The other measurements were performed in a simulated atmospheric boundary layer with varying rotor operating conditions ($\lambda = 3.5$ to $\lambda = 9.3$).
From the first series of experiments no effects could be found as to the effect of tower shape or nacelle shape on the wake depth. In all cases the wake centerline moved towards the ground plane by approximately 1.7°.
The experiments in the simulated atmospheric boundary layer show that the rotor drag and initial velocity deficit in the wake are strongly interrelated. A slight power reduction of about 5% in maximum power coefficient in the ABL-flow conditions is observed, compared to the uniform flow conditions. The results of the experiments are fully described in a data report [5].

The results of the experiments described in [5] are, among others, used to evaluate two wind turbine wake calculation models, the TNO-MILLY semi-empirical model and the CERL-NWAKE eddy viscosity model respectively.
Results of the calculation according to the MILLY model in case of very low turbulent flow ($\sigma_u \sim 0.5\%$) show that wake mixing is generally overpredicted. Calculations according to the present MILLY wake description for high turbulent flow condition ($\sigma_u \sim 11\%$) show that the wake mixing model performs satisfactory for normal operating conditions ($\lambda \approx 6.6$). At tipspeed ratio's above 6.6 the wake growth is underestimated and at lower tipspeed ratio the wake growth is overestimated.

Evaluation of the eddy viscosity model showed some inconsistencies in both the fysics and the numerical structure. As a result of this a new "ambient viscosity" and near wake model were introduced.
Results of calculation with the modified model, however, indicate that modelling of the "rotor generated viscosity" in the near wake is probably needed.

1. INTRODUCTION

Within the Netherlands National Developmentprogramme for Wind Energy (NOW fase 1) the department of fluid dynamics of TNO-Apeldoorn has carried out research on wind turbine wake flow and wake interaction e.g. [1,2,12].
As a result of these investigations the MILLY computer model has been developed to calculate the power reduction of wind farms due to wake effects [11].

Similar investigations have been carried out in several other countries. At the CERL in Leatherhead (UK) a single wake calculation model (NWAKE) has been developed based on an eddy viscosity approximation of the axisymmetric Navier-Stokes equations.
A copy of this programme has been placed at the disposal of the fluid dynamics department of TNO.

To evaluate and refine the MILLY and NWAKE models, wind tunnel measurements have been carried out. In these experiments special attention has been given to the effect of tower and nacelle as well as to the influence of turbulent shear flow on the wake mixing and power loss.
The results of these experimented investigations are presented in two reports by Talmon [4,5].

In this report these experimental results are briefly discussed (chapter 2). Furthermore these results will, among others, be used to evaluate both wake calculation models (chapter 3 and 4).

2. WIND TUNNEL EXPERIMENTS

2.1 Influence of tower and nacelle

To investigate the effects of tower and nacelle on the wind turbine wake flow Talmon [4,5] has carried out wind tunnel measurements in the wake of a 0.36 m diameter horizontal axis wind turbine (HAWT) model.

These measurements were performed in low turbulent uniform flow conditions ($\sigma_u \sim 0{,}5\%$) using a false floor to eliminate boundary layer effects.

In these experiments the rotor was placed on top of a cylindrical and a lattice tower (fig. 1). The effect of nacelle shape has been investigated using a rectangular and a cylindrical nacelle.

The rotor has been operated at a tipspeed ratio (λ) of 6.4 yielding a rotor drag coefficient (C_T) of 0.73 (fig. 2).

In fig. 2 the measured rotor drag and power coefficients are compared to the measurements performed by Vermeulen in 1978 [2]. As can be seen a considerable reduction in maximum power coefficient (C_p) is found.

Although visual inspection showed no blade damage this power reduction is probably caused by a change in rotor blade characteristics over the years.

The maximum velocity defect measured in the wake as a function of the downstream distance is given in fig. 3.

As is illustrated in fig. 4 the location of this maximum velocity deficit shifts downward by approximately 1.7°.

Talmon [4] suggests this downshift to be caused by the presence of the tower and the wind tunnel floor. The previous series of experiments (in 1978) have been carried out at the wind-tunnel center-line, i.e. at a distance of roughly 3 D from the tunnel floor. During those tests, no downshift was observed. From fig. 4 the influence of the cylindrical tower on the downshift of the wake appears to be somewhat larger compared to the lattice tower. This is probably due to the higher blockage of the oncoming flow caused by the cylindrical tower.

Due to instrumental failure the total drag of the rotor-tower-nacelle combination could not be measured. Obviously this total drag will be higher than the drag in the configuration used by Vermeulen [1] without tower.
This results in an increase of the maximum velocity defect in the wake comparced to these measurements as illustrated in fig. 3.
In the wake region beyond 4 rotordiameters downstream, the maximum velocity defect in the present experiments exeeds the deficit measured by Vermeulen to a considerable extend. As suggested by Talmon this reduced decay is probably caused by the rather small ambient turbulence compared to the flow conditions used by Vermeulen, σ_u beeing 0.5% and 1% respectively.

The correlation between the near wake length and ambient turbulence level as is shown in fig. 5 reveals that in this low turbulent flow the initial wake mixing is probably very much retarded. Between the two tower configurations, the differences in wake decay are negligible. Therefore no influence of tower configuration beyond 4 D may be concluded from the measured velocity defect, shown in fig. 3.

The nacelle shape used in this investigation does not have any measurable effect on the average flow field in the wake.

2.2 Turbulent shear flow

A second series of experiments performed by Talmon [5] consists of wake measurements behind the 0.36 m HAWT model on top of the cylindrical tower in a simulated atmosferic boundary layer (figs. 6,7). In these experiments the effect of rotor operating conditions on the wind turbine wake flow is investigated.
Wake velocities were measured while operating the rotor in a range of tipspeed ratio's varying from $\lambda = 3.5$ till $\lambda = 9.3$. The rotor operating conditions are given in table 1.
The result of the wind tunnel measurements are given in figs. 8,9.

Comparing figs. 2 and 8 shows the influence of changing flow conditions on the rotor performance of the wind turbine model. A reduction of the maximum power coefficient in simulated ABC-flow of about 5% is observed compared to the measurements in uniform flow.

From table 1 no effect on the measured drag coefficient is found. Fig. 9 shows the measured centerline velocity deficit as a function of the downstream distance at different rotor tipspeed ratio's (λ). Increasing λ leads to an increase of the velocity deficit in the wake. At higher tipspeed ratio (λ = 8.5 and 9.3) however the effect of increasing λ diminihes because of the increased wake mixing.

The rotor operating conditions however do not appear to have any noticeable effect on the centerline velocity defect rate of decay. The empirical relation established by Vermeulen [3] assuming a constant rate of decay (m = -1.25) shows to be a good approximation in turbulent shear flow as is illustrated in fig. 9.

The data report of Talmon [5] contains much more information. The reader is therefore referred to [5] for tabulated results.

3. EVALUATION OF THE MILLY MODEL

3.1 Description of the MILLY model

The MILLY wind turbine wake calculation model as developed by Vermeulen et al. [11] is based on a semi-empirical model of Lissaman and Bate [10].
In [11] an extensive description of the MILLY model is given, consequently in this report only the main features of the model will be discussed.

In the MILLY model the wake is devided into a near-, intermediate - and far wake region (fig. 10).
The first "potential core" region contains an area in which the time-averaged axial velocity according to the axial momentum theory remains constant. This potential core mixes gradually with the outer flow due to ambient turbulence as wel as shear- and rotor generated turbulence.
The length of this potential core region (X_H) therefore depends on the ambient turbulence level, rotor drag and tipspeed ratio. The empirical relations to calculate the near wake length (X_N) used in the MILLY model are described by Vermeulen [3].
Beyond the potential core region the time-averaged axial velocity profile is assumed to be self-similar.
Taking the momentum deficit to be constant and equal to the rotor drag coefficient and assuming a constant centerline velocity defect decay rate the axial velocity distribution in the wake can be calculated.

The region of constant wake width and centerline velocity deficit between X_N and X_N has been introduced in order to achieve a correct connection of the near wake and the constant decay region while taking a constant momentum deficit equal to C_T (see appendix).

In the far wake region the wake growth is defined by the ambient turbulence only. The calculation of the wake flow then is taken similar to the calculation passive contaminant dispersion in stack-plumes [10].

3.2 Evaluation in low turbulent flow

As stated in chapter 2 the results of the wind tunnel measurements presented in ref. [4] indicate that no conclusions can be drawn regarding the influence of tower and nacelle on the wind turbine wake flow.
The differences in these results compared to previous experiments are most likely to be caused by the reduced ambient turbulence and not by the presence of tower or nacelle.
Therefore no efforts have been made to incorporate any of these effects in the MILLY model.

Fig. 11 shows the calculated centerline velocity defect compared to the measurements performed in low turbulent uniform flow conditions.
Due to malfunctioning of the instruments used in the experiments no drag coefficient of the wind turbine rotor combined with tower and nacelle is known.
Assuming this total drag to be less then the drag of the separate parts added together and to exeed the drag of the rotor alone a range of C_T-values can be specificed.
Fig. 11 presents the results of calculations with the MILLY wake description using the upper and lower limit of this range.
As can be seen the decay of the centerline velocity deficit is underestimated in the region of constant decay rate ($X/_D > \sim 5.5$).
Thus in this very low turbulent flow ($\sigma_u \sim 0.5\%$) the empirical relation describing the wake mixing due to ambient turbulence appears to be inadequate.

This is illustrated by fig. 12 showing the near wake length (X_{NW}) as a function of the ambient turbulence level for the 0.36 m HAWT model for a range of tests.
As can be seen the near wake length is underestimated in the low turbulence region using the MILLY wake description.

Assuming the empirical relations describing the effect of rotor- and shear generated turbulence on the wake growth to be correct, the contribution of the ambient turbulence can be calculated from the experiments.

It shows that this method yields negative values of $(\frac{dr}{dx})_\alpha$ (table 2).

As Vermeulen [3] has pointed out the effect of this low ambient turbulence level will be very small so the calculations mentioned above probably show that the effect of rotor induced turbulence is exaggerated in those flow conditions.
Flow conditions with a turbulence level of 0.5% however are not relevant for practical use in atmospheric conditions. Therefore no efforts have been made to improve the MILLY wake description for this type of flow.

3.3 Evaluation in turbulent shear flow

A second series of wind tunnel measurements have been performed in a simulated atmosferic boundary layer. The results of these measurements are presented in chapter 2 and [5].
Figs. 13-17 present the results of calculations with the MILLY wake description for this type of turbulent flow using the rotor operating condition mentioned in table I.
Fig. 13 shows the calculated centerline velocity deficit compared to the measurements of Talmon. Fig. 14 shows the corresponding radial velocity defect profile. From this velocity defect profile the power reduction in the wake can be calculated. This is shown in figs. 16, and 17.
As can be seen in fig. 13 the near wake length (X_N) is overestimated in case of the high tipspeed ratio ($\lambda = 8.5$) while at low tipspeed ratio ($\lambda = 4.5$) X_N is somewhat underestimated.
Fig. 14 shows the calculated velocity defect profile at various distances behind the rotor area. At $\lambda = 6.6$ the MILLY calculation appears to be quite satisfactory.
From table 2 it can be found that at lower tipspeed ratio the near wake length X_N is to large compared to the experiments while at higher λ the calculated near wake length becomes to small.
To evaluate the effect of ambient turbulence as well as the rotor generated turbulence on the calculated near wake length fig. 15 has been drawn.

Here the combined effects of $(\frac{dr}{dx})_\alpha$ and $(\frac{dr}{dx})_\lambda$ are presented from both the MILLY wake description and from the calculated near wake length (X_N) according to the measured velocity deficit.

The contribution of the shear generated turbulence $(\frac{dr}{dx})_m$ is assumed to be modeled correctly [11]. It shows that at $\lambda = 6.6$, the normal rotor operating condition, the calculated and "measured" terms are approximately equal.
At higher tipspeed ratio the wake grows much faster than the MILLY model predicts while at lower tipspeed ratio the wake growth is overestimated by MILLY.

In this turbulent flow the interaction of wake and outer flow appears to be different from the MILLY description.
To create a more accurate wake flow description however use will have to be made of more fundamental and less empirical modelling techniques.

As the purpose of the MILLY model is to calculate the power loss in wind farms the available wind power in the wake has been calculated from both the wind tunnel measurements (fig. 16) and the MILLY single wake model (fig. 17). Fig. 16 shows the large effect of increasing the ambient turbulence from 0.5 tot 1% as formerly illustrated in fig. 3.
Especially at low tipspeed ratio the power ratio is overestimated according to fig. 17. As expected the power ratio is calculated quite well at $\lambda = 6.6$ in turbulent flow.
Close behing the rotor area ($y/D < 2$) the shape of the velocity distribution in the wake is influenced by the rather large nacelle so the "measured" and calculated power ratio's are different.

4. EVALUATION OF EDDY VISCOSITY MODEL

4.1 Description of the NWAKE model

The single wake calculation model has been developed at CERL by J.C. Ainslie [6,7].
In this model the thin shear layer approximation of the axisymmetric Navier-stokes equations is solved.
The turbulent stresses are assumed to be proportional to the mean velocity gradient using:

$$-\overline{uv} = \varepsilon.\frac{Du}{Dr} \qquad 4.1$$

The eddy viscosity ε then is modeled by choosing a suitable combination of length and velocity-scales

$$\varepsilon\ (x) \sim l(x)\ .\ U(x) \qquad 4.2$$

The eddy viscosity used in this model consists of two parts:

$$\varepsilon = \varepsilon_w + \varepsilon_a \qquad 4.3$$

First there is a contribution due to the shear generated turbulence within the wake (ε_w) and secondly there is a component representing the influence of ambient turbulence on the wake growth (ε_a).

The eddy viscosity due to shear is modeled as:

$$\varepsilon_w = k\ .\ b\ .\ (U_\infty - U_{cl}) \qquad 4.4$$

with k constant over the whole flowfield.

As the eddy viscosity concept is only relevant in case the turbulent flow is in local equilibrium i.e. turbulent energy production equals dissipation, the near wake can not be modeled this way.
To account for this non-equilibrium flow a filter function F(x) is introduced based upon simulator (gauze) measurements:

$$F(x) = 0.65 + (x-4.5)/23.32)^{1/3} \quad X/D < 5.5$$
$$F(x) = 1 \quad X/D \geqq 5.5 \qquad 4.5$$

The "shear viscosity" ε_w then is written as

$$\varepsilon_w = F(x).k_2.b.(U_\infty - U_{cl}) \qquad 4.6$$

The influence of ambient turbulence on the wake mixing is modeled using the turbulent velocity fluctuations ($\overline{u_a^2}$) as a suitable velocity scale. The "ambient viscosity" component ε_a is given as:

$$\varepsilon_a = k_1 . C_T . b . (U_\infty - U_{cl.}) \qquad 4.7$$

The total effective eddy viscosity becomes:

$$\varepsilon = \varepsilon_w + \varepsilon_a$$

$$= F(x) . K_2 . b . (U_\infty - U_{cl}) + k_1 . C_T . b . \frac{\overline{u_a^2}}{U_\infty - U_{cl.}} \qquad 4.8$$

Ainslie [4] suggests the factor k_2 to be 0.015. Bij fitting the calculations to simular experiments at CERL and TNO Ainslie finds the factor k_1 to depend on the length scale rotor diameter ratio (40):

	L/D	k_1
CERL	2	0.44
TNO	6	0.9

In the solution of the Navier-stokes differential equations use is made of an implicit numerical finite difference sceme. This procedure is described in detail in [6].

Calculation starts at a (minimum) distance of two rotordiameters downstream of the rotor using a Gaussian velocity defect profile.
The initial centerline velocity deficit is one of the input data for the programma and must be specified by other techniques. As this starting condition is essential, the NWAKE model therefore is incomplete as long as there is no connection between initial velocity defect and rotor operating conditions.

4.2 Evaluation of the NWAKE model

The original NWAKE algorithm written in Hewlett-Packard HP-85 BASIC has been rewritten into FORTRAN 4X and implemented in a HP-1000-F mini computer at the department of fluid dynamics of TNO.
With this programme some calculations have been made results of which are presented in figs. 18-22.
First of all a comparison was made to calculations performed at CERL [6] to check wether the translated programme was identical to the original version. The calculation showed to be identical so no translation errors were introduced.
Furthermore the model calculations are compared to various measurements. In these calculations the initial velocity defect at 2D has been fitted to the measurements.
Assuming a Gaussian velocity defect distribution the initial wake width at 2D was calculated by taking the axial momentum deficit to be equal to the thrust coefficient C_T.

Fig. 18 shows the result of the NWAKE calculation in low turbulent flow condition compared to the measurements of Vermeulen [1]. In figs. 19,20 a similar comparison is made in case of higher turbulent ABL flow as used by Talmon [5]. Fig. 21 compares calculations with the NWAKE model to full scale measurements by Baker and Walker [8].
As a result of these calculations some aspects of the NWAKE model drew attention:

- the calculated eddy viscosity rapidly increased downstream (fig. 22);
- as a result of this the wake width grew very rapidly soon exeeding the calculation grid boundary (fig. 22);
- as stated before calculation starts at a minimum distance of 2D downstream. To describe the whole wake it is neccessary to develop a new near wake calculation model to start as close to the rotor as possible.

Eddy viscosity modelling

The rapid increase of the eddy viscosity is caused by the "ambient turbulence" contribution ε_a.

Theoretical analysis of axisymmetric wakes shows that the decay of centerline velocity deficit can be written as [16]:

$$(U_\infty - U_{cl}) \sim x^{-m} \qquad 4.9$$

Conservation of momentum then leads to a calculated wake width b beeing:

$$b \sim x^{m/2} \qquad 4.10$$

assuming the velocity deficit to be small.

Vermeulen [3] states m to be 1.25 based upon measured wake data.
Eq. 4.6 then yields:

$$\varepsilon_a \sim x^{1.875} \qquad 4.11$$

Thus this "ambient" viscosity term will rapidly increase downstream. This phenomenon is felt to be highly unrealistic since the turbulent viscosity is expected to approach an ambient level at large distance downstream.
As a result of this an alternative "ambient viscosity" model is developed.

Rodi [9] states the physically most meaningfull velocity scale to be $\sqrt{k}$, k beeing the kinetic energy of turbulent motion per unit of mass. The eddy viscosity relation then can be written as:

$$\varepsilon_a = k_3 \cdot \sqrt{k} \cdot l_u \cdot \eta_1 \cdot \eta_2 \qquad 4.12$$

l_u beeing a turbulent length scale.

The efficiency factor η_1 incorporates the effect of the varying length scale ratio (l_u/b) on the wake mixing.
In absence of relevant data this efficiency factor is modeled by means of a Raleigh function.

$$\eta_1 = \exp(0.5) \{ (l_u/b) \exp(-0.5 \cdot (l_u/b)^2) \} \qquad 4.13$$

This function is presented in fig. 23.

The second efficiency factor η_2 incorporates the effect of ambient turbulence level with decreasing velocity deficit $U_\infty - U_{cl}$.
Therefore the factor η_2 is written as:

$$\eta_2 = \frac{U_{cl}}{U_\infty} \qquad 4.14$$

The "ambient" eddy viscosity then is given by:

$$\varepsilon_a = k_3 \cdot \eta_1 \cdot l_u \cdot \sqrt{k} \cdot \frac{U_{cl}}{U_\infty} \qquad 4.15$$

Wake width

The finite difference grid that is used to calculate the flow field consists of a fixed number of nodal points at equal distances at both radial and axial direction.
Therefore the maximum wake width that can be calculated equals:

$$(b)_{max} = N * \Delta r$$

N = number of no axial nodal points, Δr = axial distance between nodal points.

As in the original programme NWAKE N = 50 and Δr = 0.1 the maximum wake width becomes 5D.
In order to prevent the calculated wake width to exeed this boundary the radial stepwidth Δr is doubled as soon as the maximum wake with is reached. A further advantage of this procedure is that in this way the grid measures can be more or less adapted to the actual wake width thus enabling more accurate calculations (e.g. of the momentum deficit) because more nodal points take part in the calculation.

Near wake calculation

The original NWAKE model starts at 2D downstream with a Gaussian initial velocity defect profile.
According to the "actuator disk" theory the velocity distribution close behind the rotor area can be described by a "top hat" velocity defect distribution with an extended viscous diameter $2R_o$ beeing:

$$2R_o = \sqrt{\frac{m+1}{2}} \qquad 4.16$$

were $$m = \sqrt{\frac{1}{1-C_T}}$$

The initial velocity defect can be calculated as:

$$(U_\infty - U)\ (= U_d) = U_\infty(1 - \sqrt{(1 - C_T)}) \qquad 4.17$$

Due to the effect of pressure difference and axial turbulent momentum flux the actual initial velocity defect will be different.
Nevertheless it seemed interesting to know if the NWAKE programme would be able to handle this type of initial velocity defect profile leaving the effects of pressure difference and turbulent momentum flux to be dealt with by an adequate near wake model to be developed later on.
As is demonstrated by fig. 24, starting with a "top-hat" velocity defect distribution the programme gradually calculates the well known "bell" shaped velocity distribution.

In order to evaluate the modifications as mentioned before some calculations have been performed with a new model EVMOD in which the following modifications are incorporated:

- new ambient viscosity model;
- ajustable radial grid size;
- axial momentum initial velocity deficit.

4.3 Results of modified model EVMOD

The results of calculations with the modified NWAKE model EVMOD are presented in figs. 25-28.
First some calculations were made in case of low turbulent flow as described in [1] (case 3).
In this low turbulent flow the contribution of the "ambient viscosity" (ε_a) will be negligible so the eddy viscosity will be determined by the "shear" contribution (ε_w).
Increasing the turbulent viscosity constant k_2 to 0.06 gives a centerline velocity defect as depicted in fig. 25. This increase in viscosity constant compared to the gauze-value of 0.015 suggested by Ainslie [6] probably indicates the effect of rotor-induced turbulence in the near wake region. As can be seen the calculated decay rate is in agreement with the empirical value of -1.25 (Vermeulen [3]).

Using this viscosity constant $k_2 = 0.06$ some calculations were carried out for the turbulent flow conditions as described in [5].
Figs. 26,27 show the effect of varying ambient turbulence level on the calculated velocity deficit in the wake.
In this calculation the turbulent interaction factor k_3 has arbitrarity chosen to be 0.1. Varying this factor will have the same effect as changing the ambient turbulence level since ε_a is determined by the combination $k_3 * \sqrt{k}$.
Fig. 26 therefore is merely a qualitative illustration of the effect of ambient turbulence on the calculated wake mixing.
Figs. 27,28 illustrate the effect of increasing the interaction factor k_3 on the calculated "ambient" eddy viscosity contribution as well as the total eddy viscosity calculated.
As a result of the relation between calculated velocity defect, wake width and corresponding eddy viscosity it is rather difficult to estimate the effect of changing one of the constants k_1 or k_3, the filter function F(x) or even introducing an extra eddy viscosity term incorporating the effect of rotor induced turbulence.
Despite this it seems appropriate to account for the effect of rotor induced turbulence. One of the possibilities to do so is to create an extra eddy viscosity relation calculating the "rotor induced viscosity" (ε_λ). In the NWAKE model an empirical filter function has been applied to account for the non-equilibrium flow close to the rotor area (eg. 4.5).

As this equation is qualitatively based on gauze measurements this filter function could possibly be modified in order to incorporate the effect of rotor turbulence.

In the present evaluation of the NWAKE model no attempts have been made to do so.

This near wake modelling however wil be part of investigations to be carried out in the future.

5. CONCLUSIONS

5.1 Wind tunnel experiments

- From the wind tunnel experiments presented in this report, no effect of the wind turbine tower and nacelle on the velocity deficit in the wake can be found.
- The present wake experiments in uniform, low turbulent flow conditions, show that the wake centerline moves towards the wind tunnel floor with increasing downstream distance, at an inclination of ca. 2°.
- The experiments with varying rotor operating conditions in a simulated atmospheric boundary layer show the rotor drag and initial velocity deficit in the wake to be strongly interrelated.

5.2 MILLY evaluation

- In uniform low turbulent flow ($\sigma_u \sim 0.5\%$), wake mixing is overestimated by the present MILLY wake description. This type of flow however is not relevant for practical application purposes.
- Calculations according to the present MILLY wake description for high turbulent flow conditions ($\sigma_u \sim 11\%$) show that the wake mixing model performs satisfactory for normal operating conditions near optimum power coefficient ($\lambda \approx 6.6$). At higher tipspeed ratio's the wake growth is underestimated while at lower tipspeed ratio's the wake growth is overestimated.

5.3 NWAKE evaluation

- From an analysis of the CERL-NWAKE model the following conclusions have been drawn:
  * The contribution of the ambient turbulence of the total eddy viscosity increases to infinity with increasing downstream distance; this behaviour is unrealistic.

* The calculated wake width exeeds the grid boundary.
* The model is not able to predict the initial velocity deficit in the near wake from the rotor operating conditions. It can therefore only be used as a practical design tool in case it is extended with a near wake model.

- The NWAKE model has been modified according to physically more realistic eddy viscosity modelling.
  Calculations with the modified model however show that some kind of empirical "rotor generated viscosity" must be introduced in the near wake.

6. REFERENCES

[1] Vermeulen, P.E.J.
Studies of the Wake Structure of Model Wind Turbine Generators.
MT-TNO Report 79-012904, November 1979.

[2] Vermeulen, P.E.J.
A Wind Tunnel Study of the Wake of a Horizontal Axis Wind Turbine.
MT-TNO Report 78-09674, September 1978.

[3] Vermeulen, P.E.J.
An experimental Analysis of Wind Turbine Wakes.
3rd International Symposium on Wind Energy Systems, Copenhagen,
August 1980.

[4] Talmon, A.M.
A Wind Tunnel Investigation into the Effects of Tower and Nacelle on Wind Turbine Wake Flow (in Dutch).
MT-TNO Report 84-08479, July 1984.

[5] Talmon, A.M.
The Wake of a Horizontal-Axis Wind Turbine Model;
Measurements in uniform Approach Flow and in a Simulated Boundary Layer (Data Report).
MT-TNO Report 85-01021, August 1985.

[6] Ainslie, J.F.
Development of an Eddy viscosity Model of a Wind Turbine Wake.
CERL-memorandum TPRD/L/AP/0081/M83, May 1983.

[7] Ainslie, J.F.
Development of an Eddy viscosity Model for Wind Turbine Wakes.
7th BWEA conference 1985.

[8] Baker, R.W., Walker, S.N.
Wake Measurements Behind a Large Horizontal Axis Wind Turbine Generator.
Solar Energy Vol. 33, no. 1 p.p. 5-12, 1984.

[9] Rodi, W.
Turbulence Models and their Application in Hydraulics - a state of the Art Review.
IAHR-paper, June 1980.

[10] Lissaman, P.B.S., Bate, E.R.
Energy Effectiveness of Arrays of Wind Energy Conversion Systems.
Aero Vironment Report AVFR 7058, Pasadena, USA (1977).

[11] Vermeulen, P.E.J., Builtjes, P.J.H., Vijge, J.B.A.
Mathematical Modelling of Wake Interaction in Wind Turbine Arrays Part I & II.
MT-TNO Report 81-01473, 81-02834, 1981.

[12] Builtjes, P.J.H.
Wind Turbine Wake Effects.
MT-TNO Report 79-08375, Augsuts 1979.

[13] Clayton, B.R., Filby, P.
Wind turbine Wake Studies.
Proc. 3rd BWEA Wind Energy conference, Cranfield 1981.

[14] Schlichting, H.
Boundary Layer theory.
McGraw-HILL, New York, 1979.

Table 1 Rotor operating conditions used in the experiments of Vermeulen (1978) and Talmon (1985)

λ	C_T (Vermeulen 1978)	C_T (Talmon, unif. flow)	C_T (Talmon, ABL)
3.5	-	-	0.42
4,5	-	-	0.52
5.0	0.61	-	-
6.6	0.74	0.73-0.79*	0.74
8.5	0.85	-	0.81
9.3	-	-	0.87

* range of C_T estimated from experiments

Table 2 Calculation of the near wake length according to MILLY

Uniform flow conditions	m	R_o	$(\frac{dr}{dx})_m$	$(\frac{dr}{dx})_\lambda$	$(\frac{dr}{dx})_\alpha$	X_N
λ = 6.4	1.92	0.60	-0.060	0.154	0.025	5.4
C_T = 0.73-079						
$\sigma_u \cong$ 0.005	2.18	0.63	-0.073	0.154	0.025	5.6

Near wake length "measured" at m = 2.18 : X_N = 6.9

$$\Rightarrow (\frac{dr}{dx})^2_\alpha = (\frac{nR_o}{X_N})^2 - ((\frac{dr}{dx})^2_\lambda + (\frac{dr}{dx})^2_m) = -0.0098$$

Table 2 Calculation of the near wake length according to MILLY

ABL- flow conditions	λ	m	R_o	$(\frac{dr}{dx})_m$	$(\frac{dr}{dx})_\lambda$	$(\frac{dr}{dx})_\alpha$	X_{nw}	(X_N) measured
σ_u = 0.11	9.3	2.77	0.69	-0.10	0.22	0.325	2.71	1.91
	8.5	2.29	0.64	-0.08	0.20	0.325	2.51	2.15
	6.6	1.96	0.61	-0.06	0.16	0.325	2.48	2.46
	4.5	1.47	0.56	-0.03	0.11	0.325	2.38	2.82
	3.5	1.31	0.54	-0.02	0.08	0.325	2.34	2.58

APPENDIX : LISSAMAN/MILLY WAKE MODEL IN REGIONS I AND II

Dahlberg and Meyer of FFA mentioned that the integrated momentum deficit in Region I does not equal the rotor thrust [1].
This can easily be shown by looking at $X = X_H$, i.e. at the end of Region I. Here, the profile is described by equation A-12 ([2])

$$\frac{\Delta U}{U_\infty} = \frac{m-1}{m} (1 - \eta^{1.5})^2 \qquad (1)$$

with $\eta = \frac{R}{R_H}$; $(R_o\ (x) = 0!)$ (2)

Because $r_H = \frac{b}{0.441}$, equation A-12 is exactly the same as eq. 3 of [2]. Conseququently the integrated momemtum deficit equals (according to eq. 4 of [3]):

$$(C_T)_{integrated} = (\frac{b}{R})^2 (2.64 \frac{\Delta Uc}{U_\infty} - 1.37 (\frac{\Delta Uc}{U_\infty})^2) \qquad (3)$$

$$\text{or } (C_T)_{integrated} = (0.881\ R_H)^2 (2.64 \frac{\Delta Uc}{U_\infty} - 1.37 (\frac{\Delta Uc}{U_\infty})^2) \qquad (4)$$

At the end of Region 1, $\frac{\Delta Uc}{U\infty}$ still equals $(\frac{\Delta Uc}{U_\infty})_{x=0} = \frac{m-1}{m}$

When R_H is calculated using eg. A-10 of [2] is follows that:

m	C_T	$(R_H)_{eg.\ A-10}$	$(C_T)_{integrated\ at\ X_H}$
1.5	0.556	0.853	0.411
2	0.75	0.865	0.567
3	0.889	0.883	0.697
5	0.960	0.914	0.801

It indeed shows that at $X = X_H$, large errors occur in the integrated deficit; the wake is too narrow.

At the same time, however, the integrated momentum deficit at $X=X_N$ is correct (and also at X = 0).

When the Lissaman/MILLY equations are used (i.e. A-3, A-10, A-13, A-16 and A-17) we see the following:

m	C_T	η	$\frac{R_N}{R_o}$	$\frac{m-1}{m}$	$\frac{\Delta Uc}{U_\infty}$	$(C_T)_{\text{integrated at } X_N}$
1.5	0.556	1.46	1.77	0.333	0.333	0.552
2	0.75	1.50	1.62	0.5	0.499	0.744
3	0.889	1.66	1.41	0.667	0.652	0.882
5	0.960	4.37	1.24	0.8	0.572	0.953

So, at $X = X_N$ and beyond the integrated momentum deficit is correct. For some reason, the equations for the <u>end</u> of Region II are correct, while between $X = 0$ and $X = X_N$ they are not.
In [4] Lissaman himself already mentions this problem.

Two further remarks can be made.

- The fact that the equations are correct at $X = X_N$ means that the whole wake calculation downwind of $X = X_N$ is also correct; because at each stage momentum conservation is used to relate velocity deficit and wake radius.
- The table shows, at least for $m \leqq 3$, that the centerline velocity deficit is almost constant from $X = 0$ to $X = X_N$.
  In [3] Vermeulen used this fact (page 439) to equate the Lissaman X_N to his $X_{N.W.}$.
  In the MILLY/Lissaman model, the centerline deficit is therefore (for $m \leqq 3$) almost constant over the first 2 regions.
  As the profile shape at $X = X_H$ equals $X = X_N$, momentum conservation therefore requires that R_H should be the same as R_N.

The FFA modification

Dahlberg and Meyer find for R_H:

$$R_H = \tfrac{1}{4} \sqrt{\frac{m+1}{m(I_1 - I_2) + I_2}} \qquad (5)$$

with $I_1 = \frac{9}{70}$

$I_2 = \frac{243}{3640}$

or $$R_H = \tfrac{1}{4} \sqrt{\frac{m+1}{0.0618\ m + 0.06676}} \qquad (6)$$

This equation is exactly similar to the above mentioned eq. 4.

When C_T and $\frac{\Delta Uc}{U_\infty}$ are expressed in terms of m, one will find of course the same equation as eq. 6.

So therefore eq. A-10 of MILLY is wrong and may be replaced by eq. 6. However, if A-10 in the MILLY model is replaced with eq. 6, everything goes wrong downwind of X_H.

Because of equations A-14 and A-15, the R_N grows and when using eq. A-16 large errors in the momentum deficit are introduced àand the centerline deficit at $X = X_N$ no longer equals $\frac{m-1}{m}$.

As already suggested above (and also on page 445 of [3]) the correct wake calculation essentially starts at $X = X_N$ and everything between $X = 0$ and $X = X_N$ is more or less used as a "black box".

The equations on page 445 of [3] give practically the same results as the "black box" of Lissaman/MILLY as long as $m \leqq \approx 3$.

So, in conclusion, an improvement of the model for Regions I and II is needed, which does not affect the present calculations for Regions III and IV.

A correct solution for regions I and II

A formal correct solution could be to replace eq. A-10 [2] with the above mentioned eq. 6, ànd to replace A-14 with:

$$R_2 (x) = R_H$$

i.e. keep the wake radius constant over Region II.
When we do this, there is (apart from nostalgia) no reason to retain equation A-16.
It is more in line with [3] to replace A-16 with:

$$\left(\frac{\Delta Uc}{U_\infty}\right)_{x_N} = \frac{m-1}{m}$$

With this modification, the flow structure does not change between $X=X_N$ and $X = X_H$, which seems rather unrealistic.
Another solution could be to adapt the form of the wake profile in Region I such that momentum conservation is retained.

Of course, a really good model for Regions I and II should be based on a more realistic description of the aerodynamics of the near wake region. Nevertheless it seems that the above suggested changes form an improvement of the MILLY model, for instance because they may partly remove the "bumps" in figure 3 of [4]. The modification has been used to recalculate fig. 3 of [4], which is shown in fig. A-2.
The "bumps" have indeed disappeared, although a "plateau" remains. This plateau of course is Region II.

Conclusions

The equations of Regions I and II should indeed be modified. A simple modification is proposed, which is, however, not based on any aerodynamic description of the near wake behaviour.

The above suggested changes will be implemented and calculations will be made to supplement the results of [4].

References

[1] Dahlberg, Meyer Vermeulen — personal communication 1984

[2] Vermeulen, Vijge — MILLY description (MT-TNO 81-02834) (equal to [11] of main report)

[3] Vermeulen — Copenhagen (BHRA Conf., paper 1980) (equal to [3] of main report)

[4] Alfredson, Dahlberg, Vermeulen — Wind Engineering 1982

Model configurations.

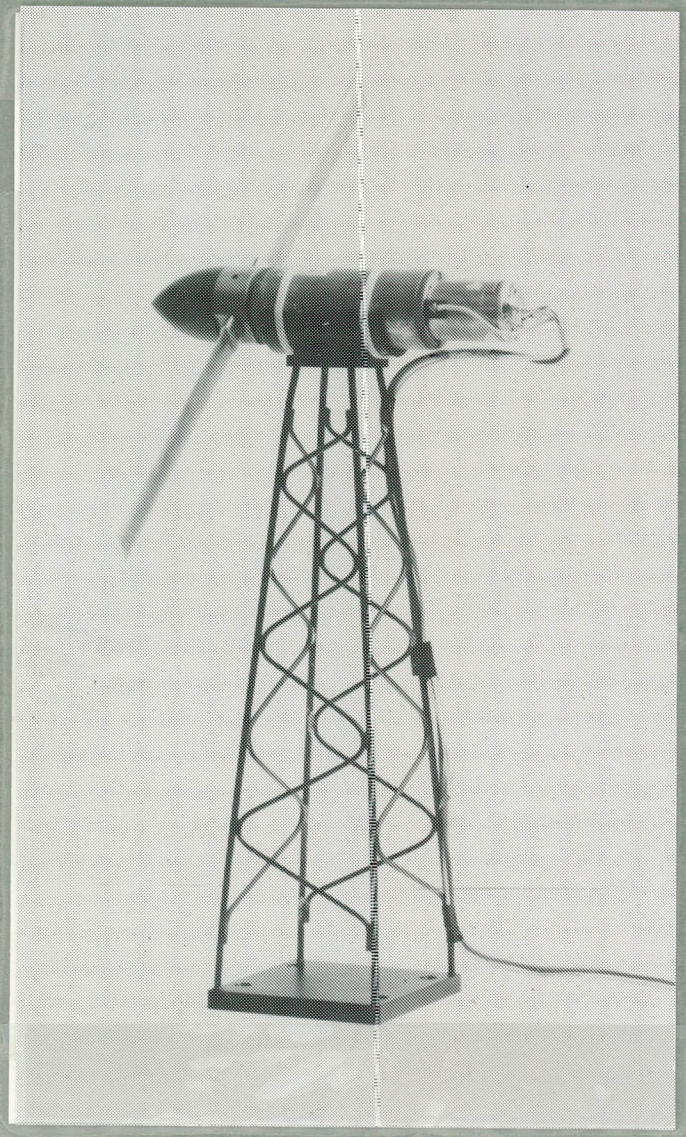

cylindrical tower,
cylindrical nacelle

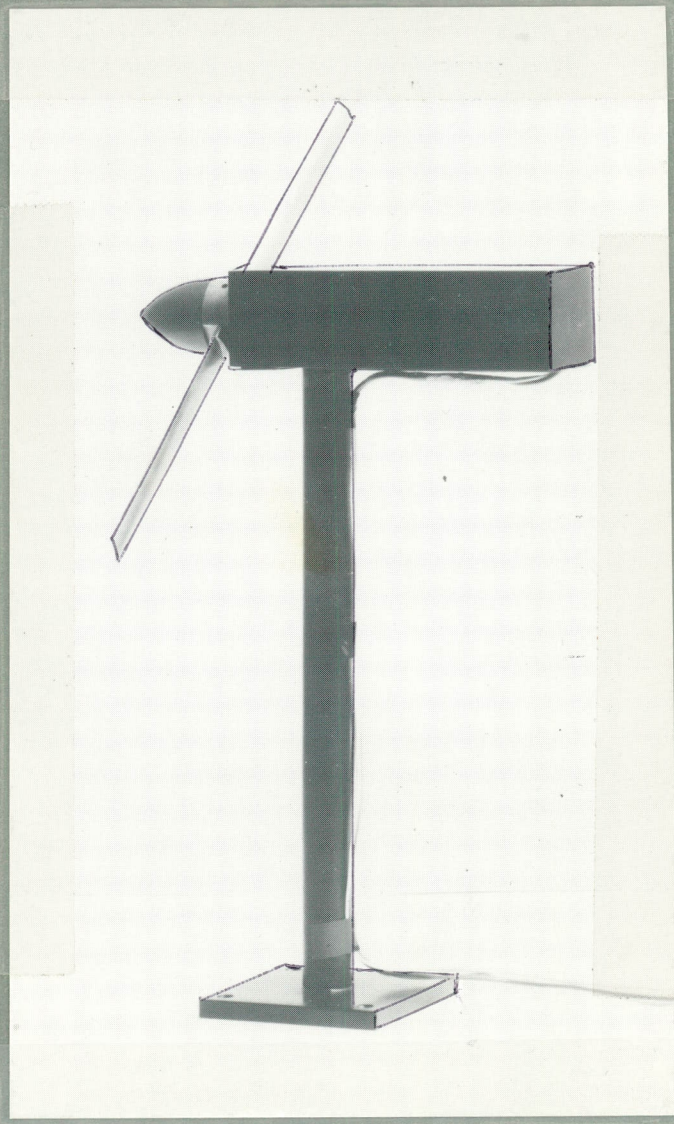

cylindrical tower,
rectangular nacelle

MT_TNO
12433
Fig. 1

cylindrical nacelle
cylindrical tower

cylindrical nacelle
rectangular tower

Model configurations.

MT_TNO
12433
Fig. 1

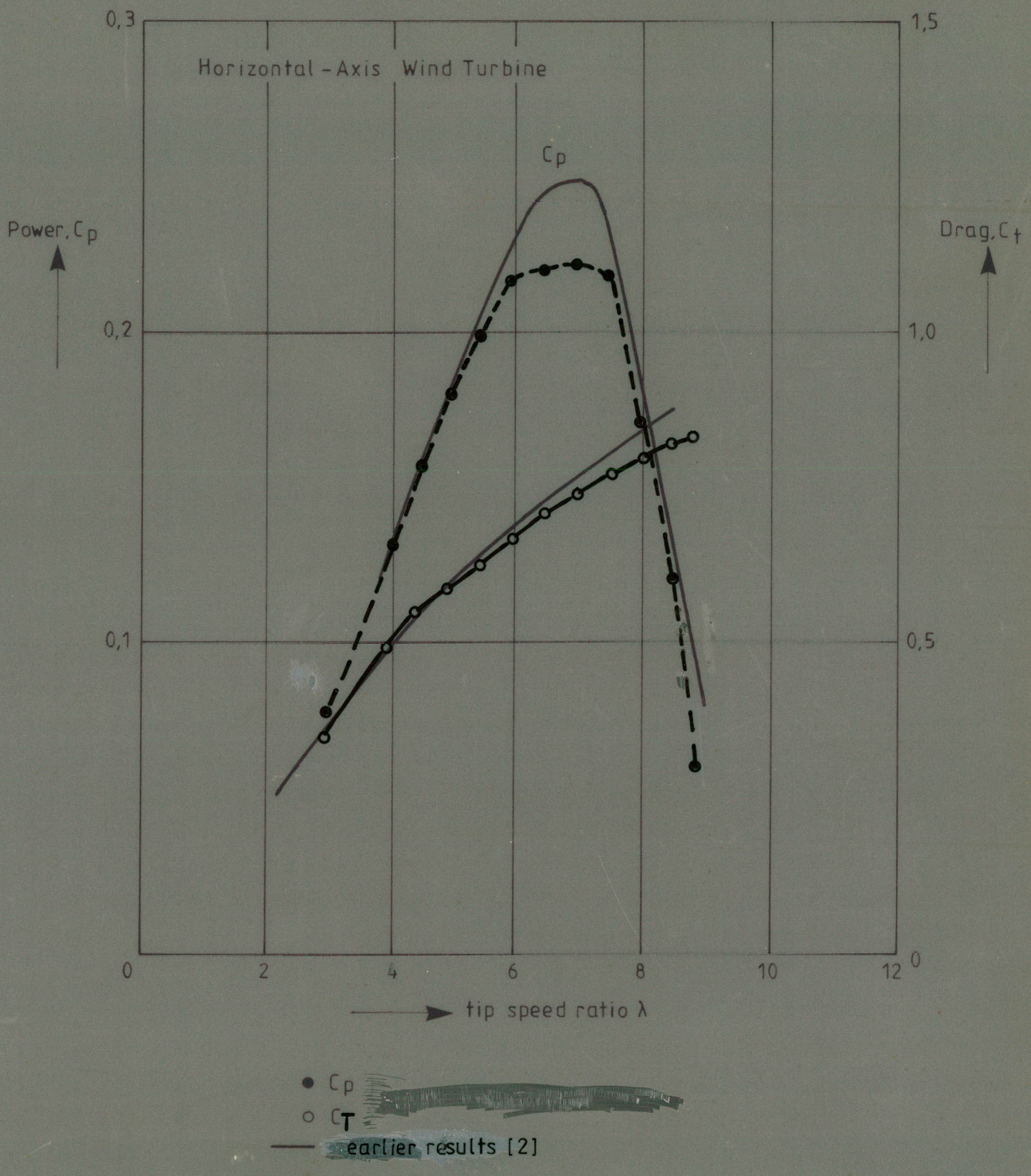

Power and Drag of the horizontal axis machine as a function of the tip-speed ratio at Ur = 9,7 m/s in uniform flow.

MT_TNO
12433
Fig. 2

Power and Drag of the horizontal axis machine as a function of the tip-speed ratio at Ur=37 m/s in uniform flow.

MT_TNO
1243
Fig.2

Maximum velocity defect decay.

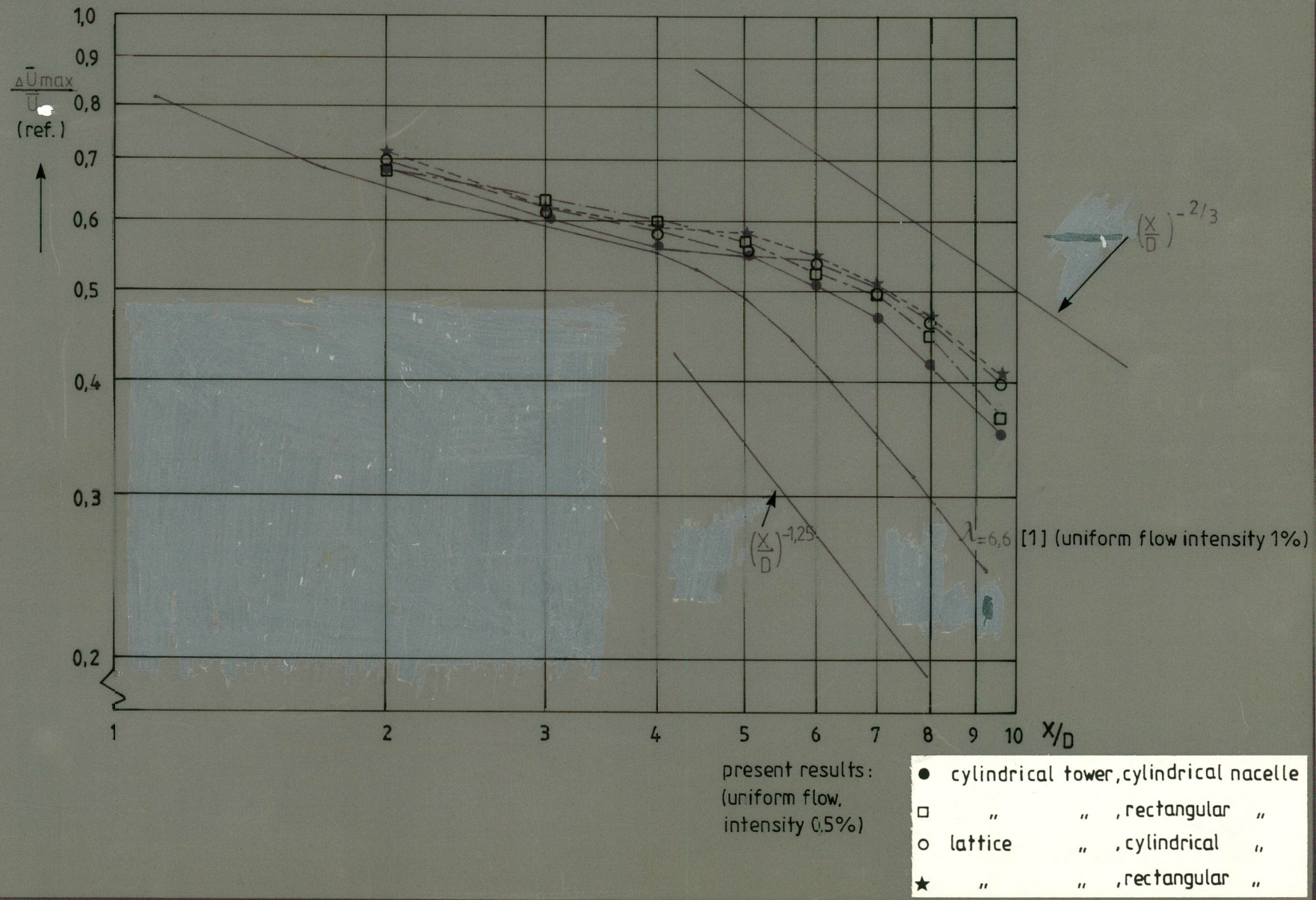

MT-TNO
12433
Fig. 3

MT-TNO
Fig. 22
Maximum velocity defect decay.

present results:
(uniform flow,
0.2° intensity)

(0.1° intensity uniform flow) [1] $\lambda = 0.8$

$(\frac{x}{D})^{-1.5}$

$(\frac{x}{D})^{-2.5}$

$\frac{x_{DM}\bar{U}_A}{U_\infty}$ (.197)

x/D 0 1 2 3 4 5 6 7 8 9 10

1.0 2.0 3.0 4.0 5.0 6.0 7.0 8.0 9.0

Wake position as a function of downstream distance

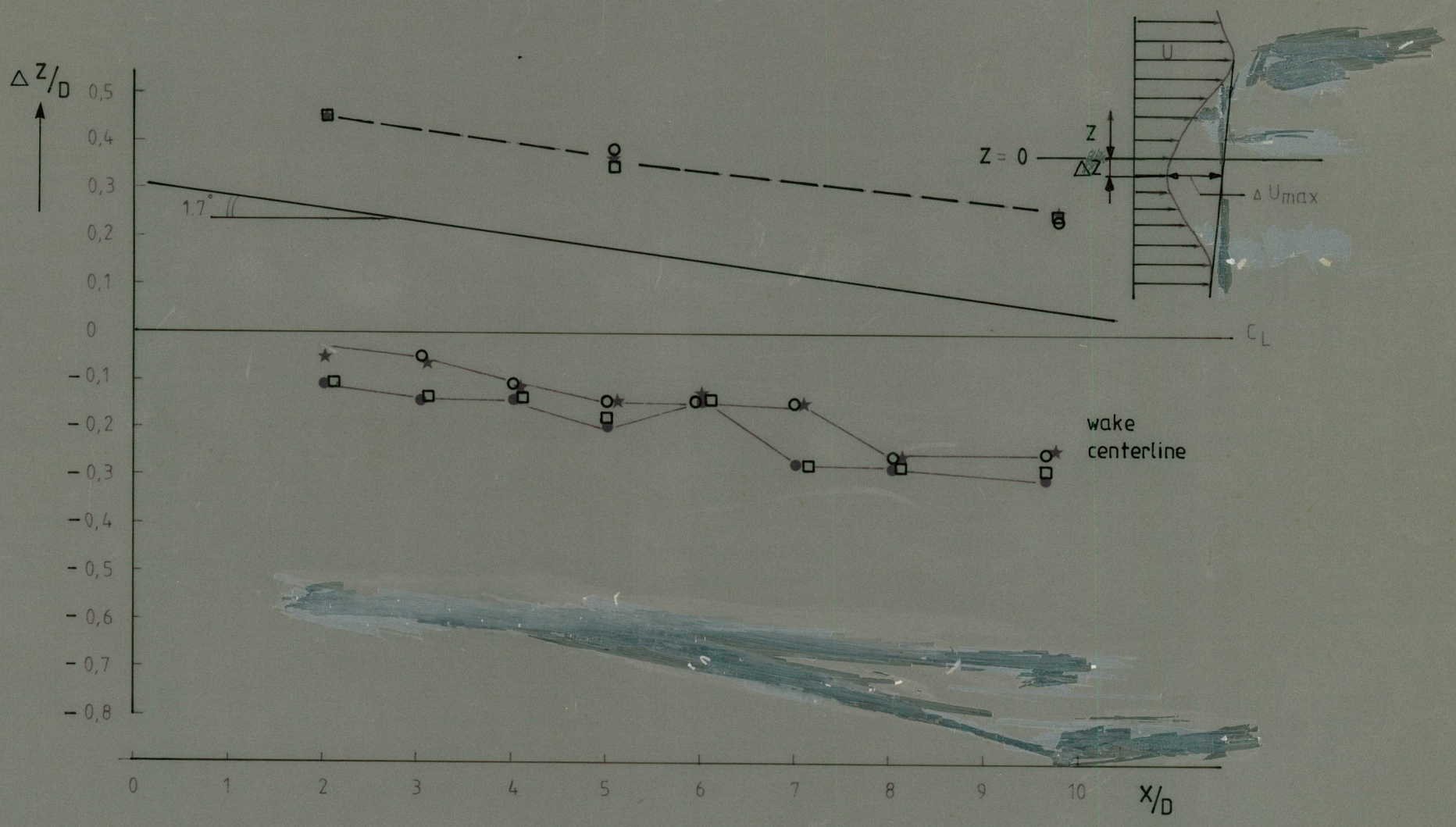

MT - TNO
12433
Fig. 4

Wake position as a function of downstream distance

Fig. 4
JSA 33
MT - TNO

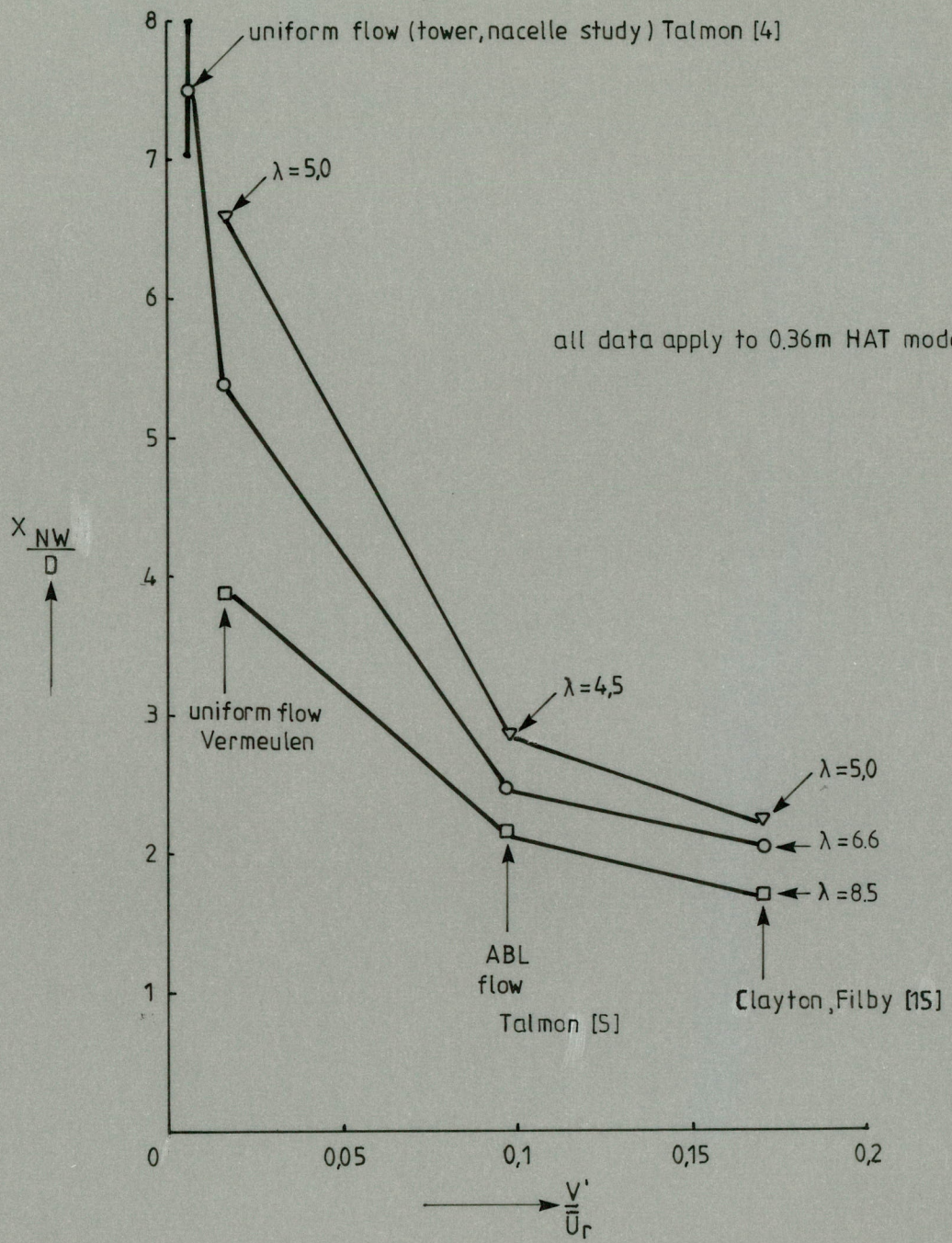

Correlation between turbulence intensity and near wake length

MT _TNO
12433
Fig. 5

Correlation between turbulence intensity and near wake length

MT_TNO
12433
Fig.5

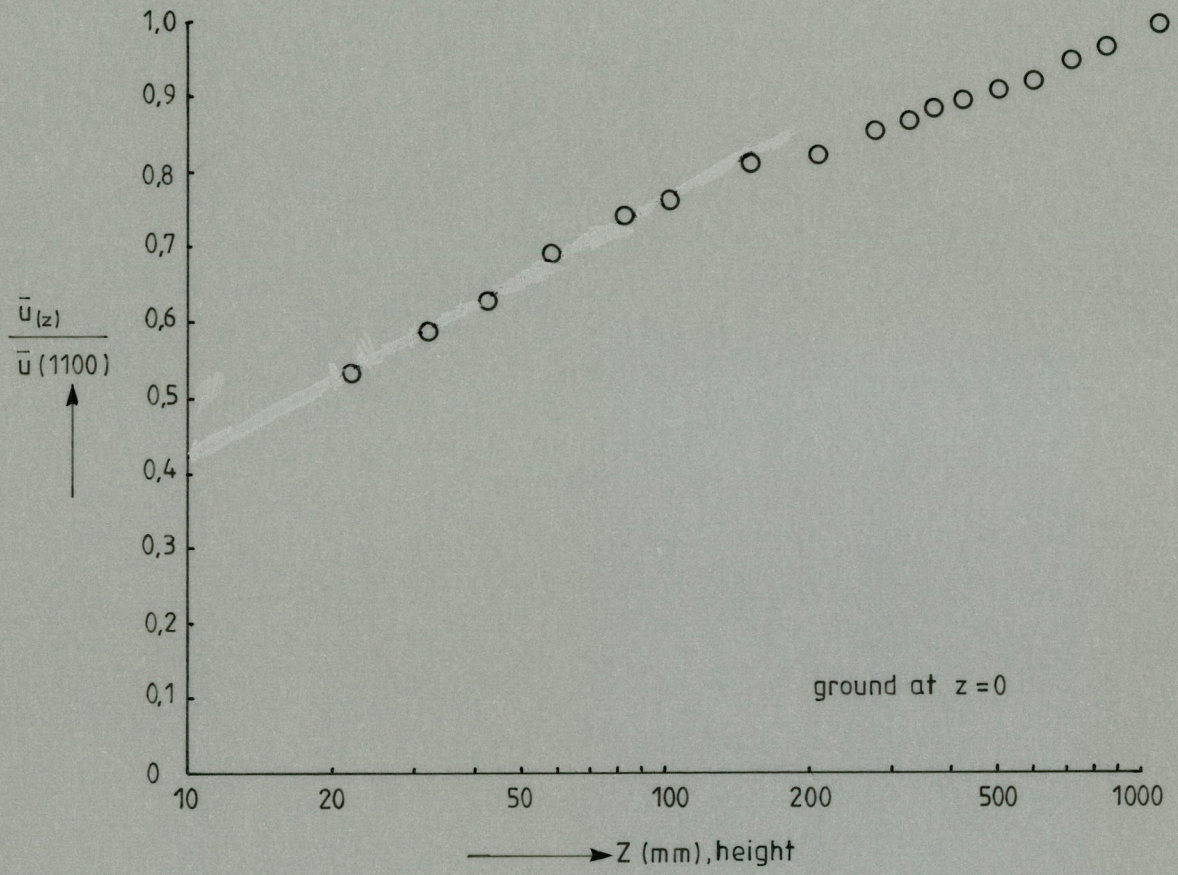

The vertical velocity profile in the ABL flow

MT_TNO
12433
Fig.6

The vertical velocity profile in the ABL flow

MT_TNO
12433
Fig.6

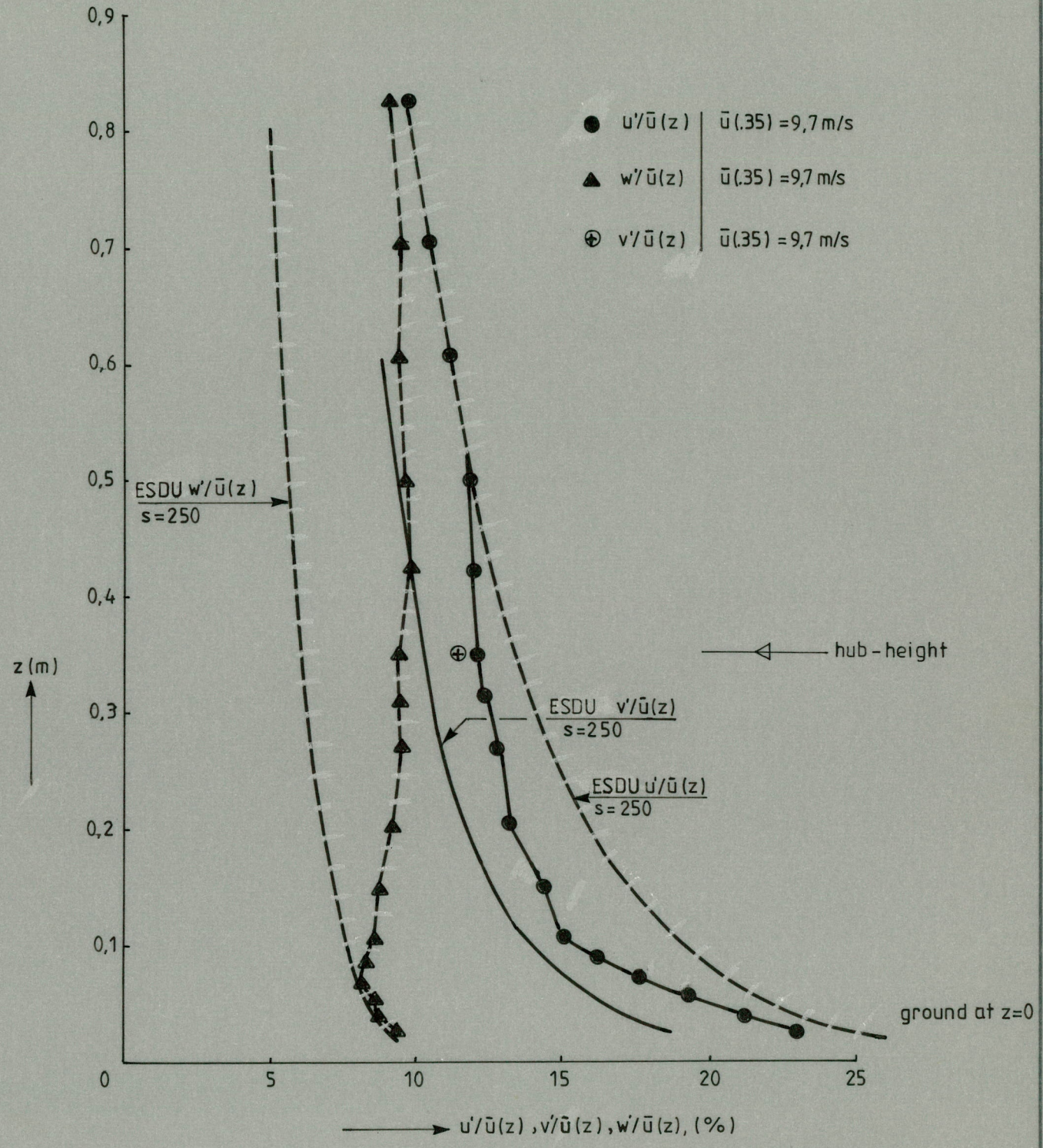

Turbulence intensities in the ABL flow

MT_TNO
12433
Fig.7

Turbulence intensities in the ABL flow

MT_TNO
12433
Fig.7

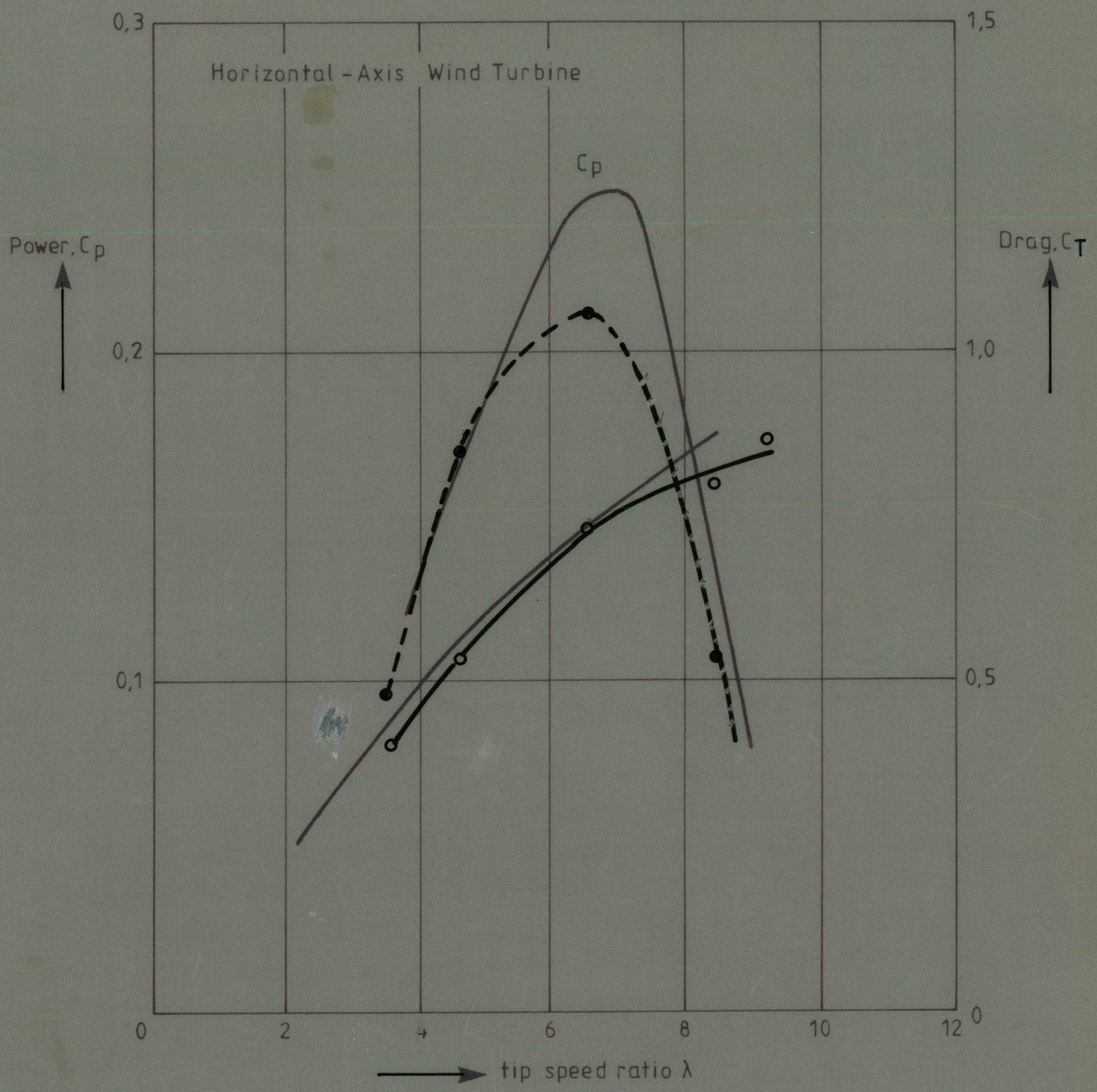

λ	Cp	Ct
3,5	0,099	0,42
4,7	0,165	0,55
6,6	0,213	0,74
8,5	0,111	0,81
9,3	–	0,87

Power and Drag of the horizontal axis machine as a function of the tip-speed ratio in ABL flow.

MT_TNO
12433
Fig. 8

λ	Cp	C_t
3,5	0,099	0,42
4,7	0,165	0,55
6,6	0,213	0,74
8,5	0,111	0,81
9,3	–	0,87

Power and Drag of the horizontal axis machine as a function of the tip-speed ratio in ABL flow.

MT_TNO
12433
Fig. 8

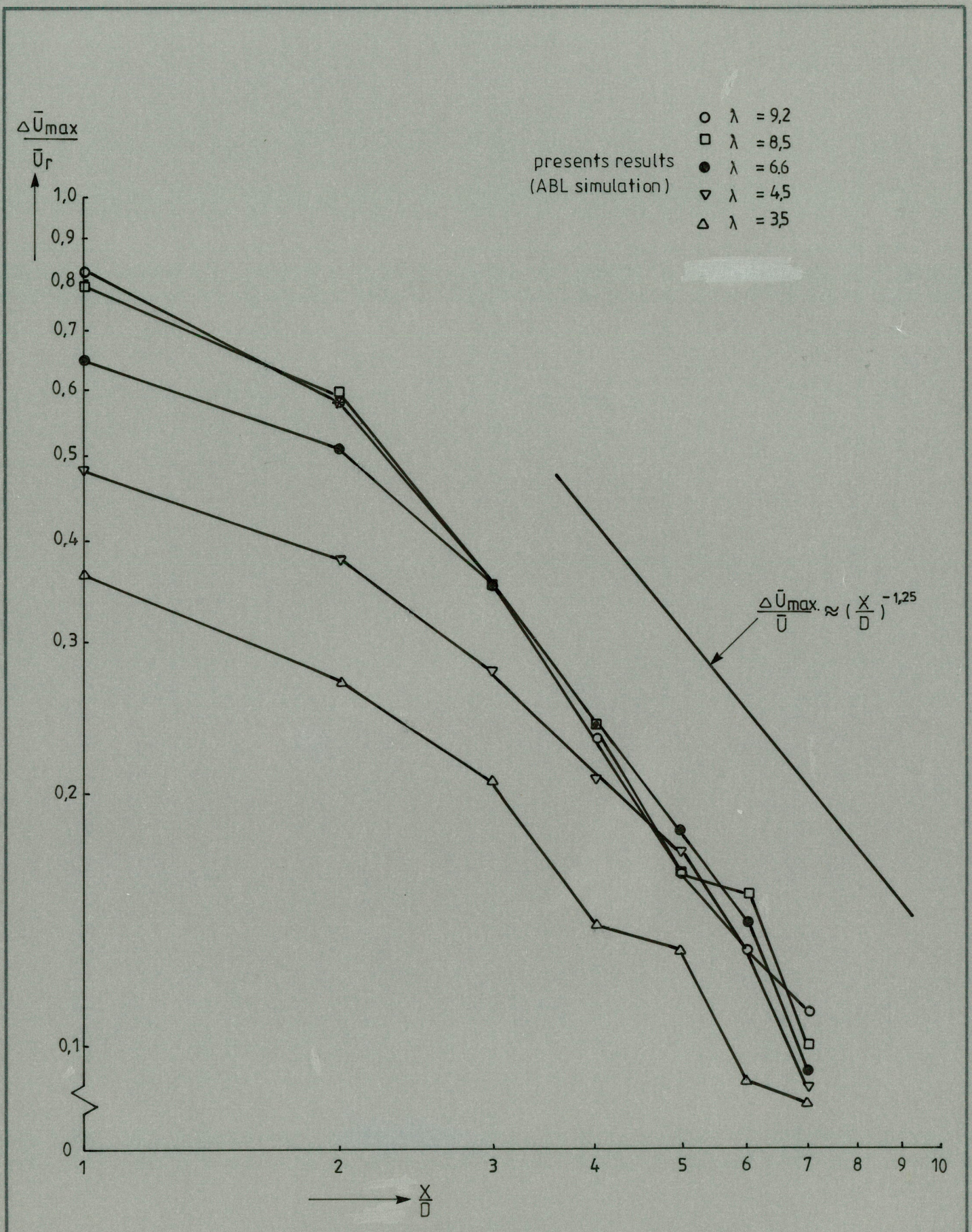

Centerline velocity defect decay

MT_TNO
12433
Fig. 9

Centerline velocity defect decay

MT_TNO
12433
Fig. 9

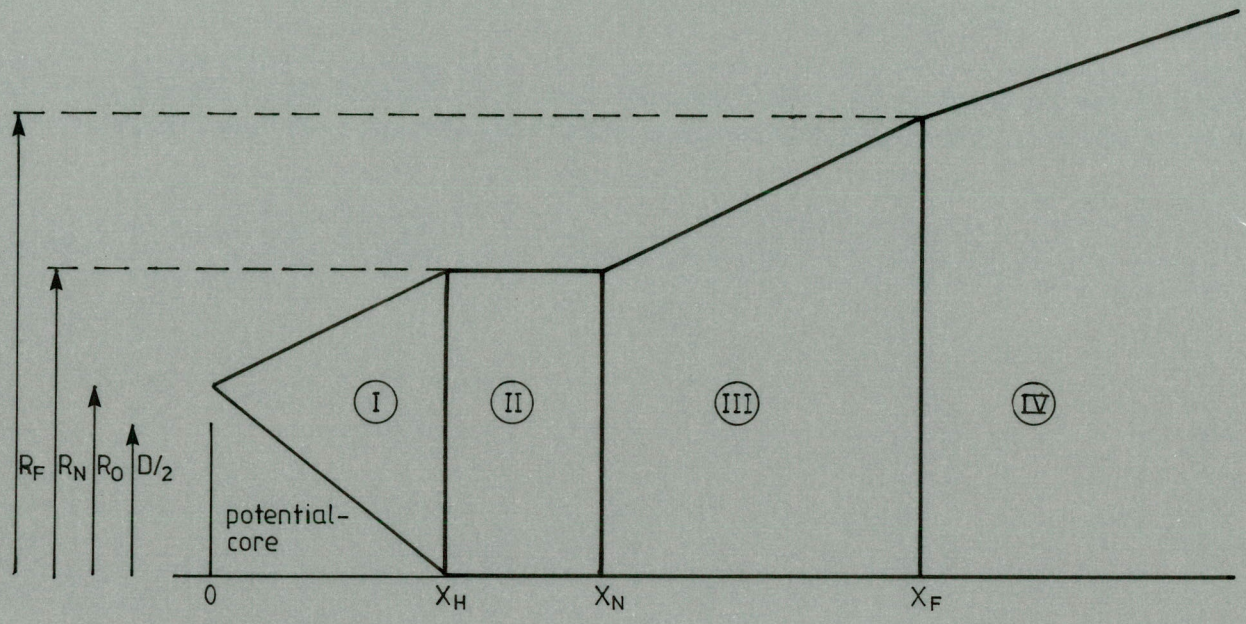

a: wake radius

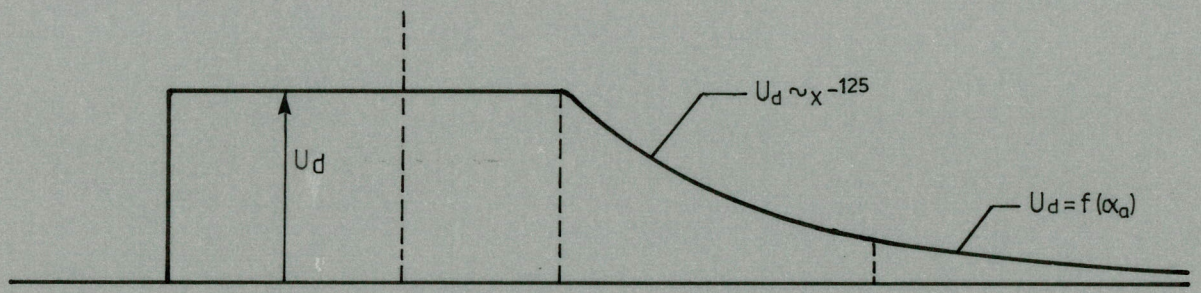

b: centerline velocity deficit

Milly windturbine wake description	MT_TNO 12433 Fig.10

a: wake radius

b: centerline velocity deficit

Milly windturbine wake description

MT_TNO
12433
Fig.10

$$P/P_o = \frac{1}{\pi R^2 . \frac{1}{2} \rho U_{ref.}^3} \int_0^R 2\pi r . \frac{1}{2} \rho U^3 dr$$

$$P/P_o = \frac{1}{\frac{1}{2} \rho U_{ref}^3 R} \int_{-R}^{R} \frac{1}{2} \rho U^3 dy \quad (ABL\_flow; ref.5)$$

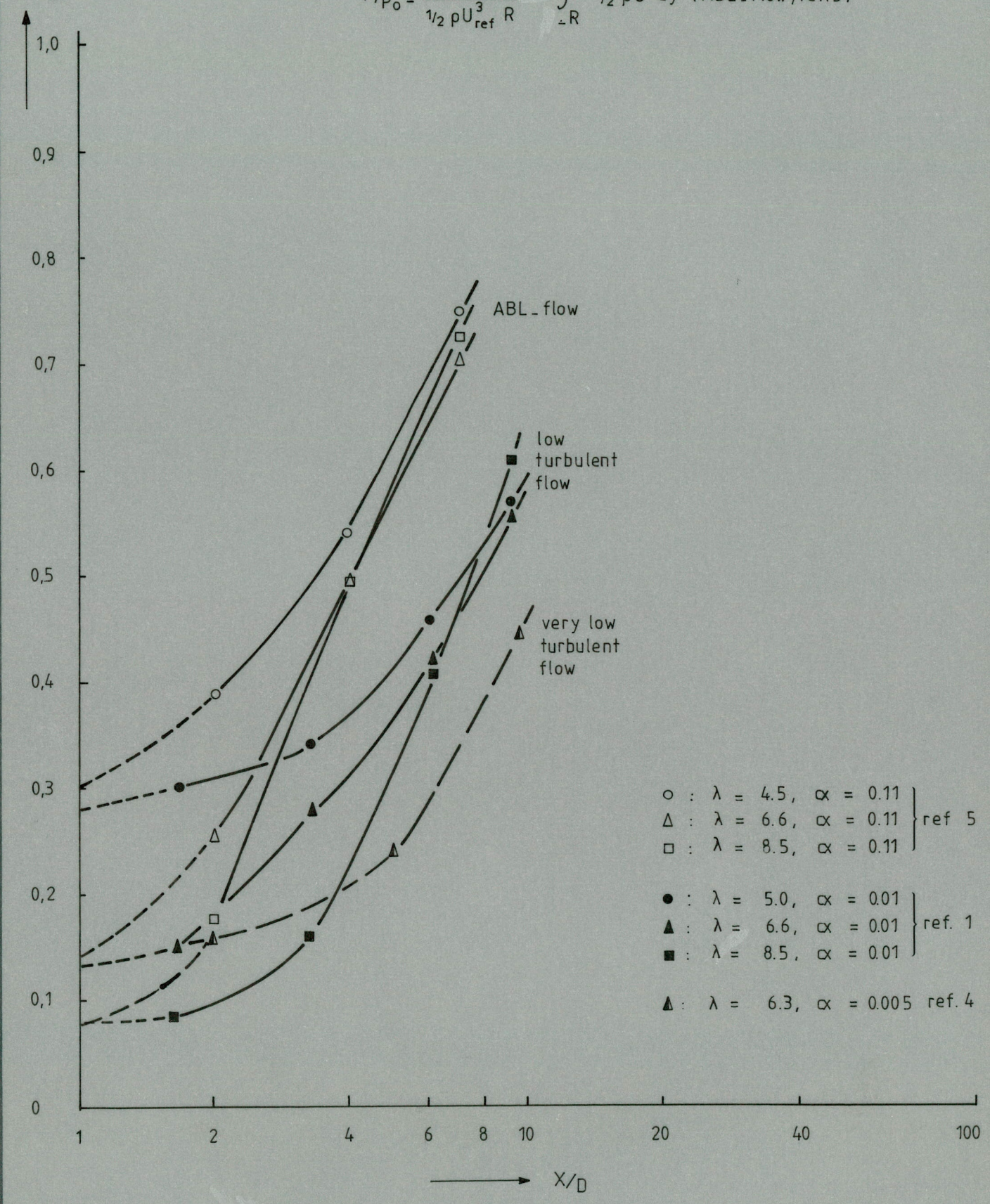

Power ratio as a function of the downstream distance at different turbulence levels

MT_TNO
12433
Fig. 16

$$P/P_\infty = \frac{1}{\frac{1}{2}\rho U_{ref}^3 R} \int_{-R}^{R} \frac{1}{2}\rho U^3 dy \quad \text{(ABL\_flow; ref.5)}$$

$$P/P_\infty = \frac{1}{\pi R^2 \cdot \frac{1}{2}\rho U_{ref}^3} \int_{0}^{R} 2\pi r \cdot \frac{1}{2}\rho U^3 dr$$

power ratio
P/P_∞

1,0
0,9
0,8
0,7
0,6
0,5
0,4
0,3
0,2
0,1
0

ABL_flow

low turbulent flow

very low turbulent flow

○ : λ = 4.5, α = 0.11
△ : λ = 6.6, α = 0.11 } ref 5
□ : λ = 8.5, α = 0.11

● : λ = 5.0, α = 0.01
▲ : λ = 6.6, α = 0.01 } ref. 1
■ : λ = 8.5, α = 0.01

▲ : λ = 6.3, α = 0.005 ref. 4

1 2 4 6 8 10 20 40 100

X/D

Power ratio as a function of the downstream distance at different turbulence levels

MT_TNO
12433
Fig.16

Symbols : see fig.16

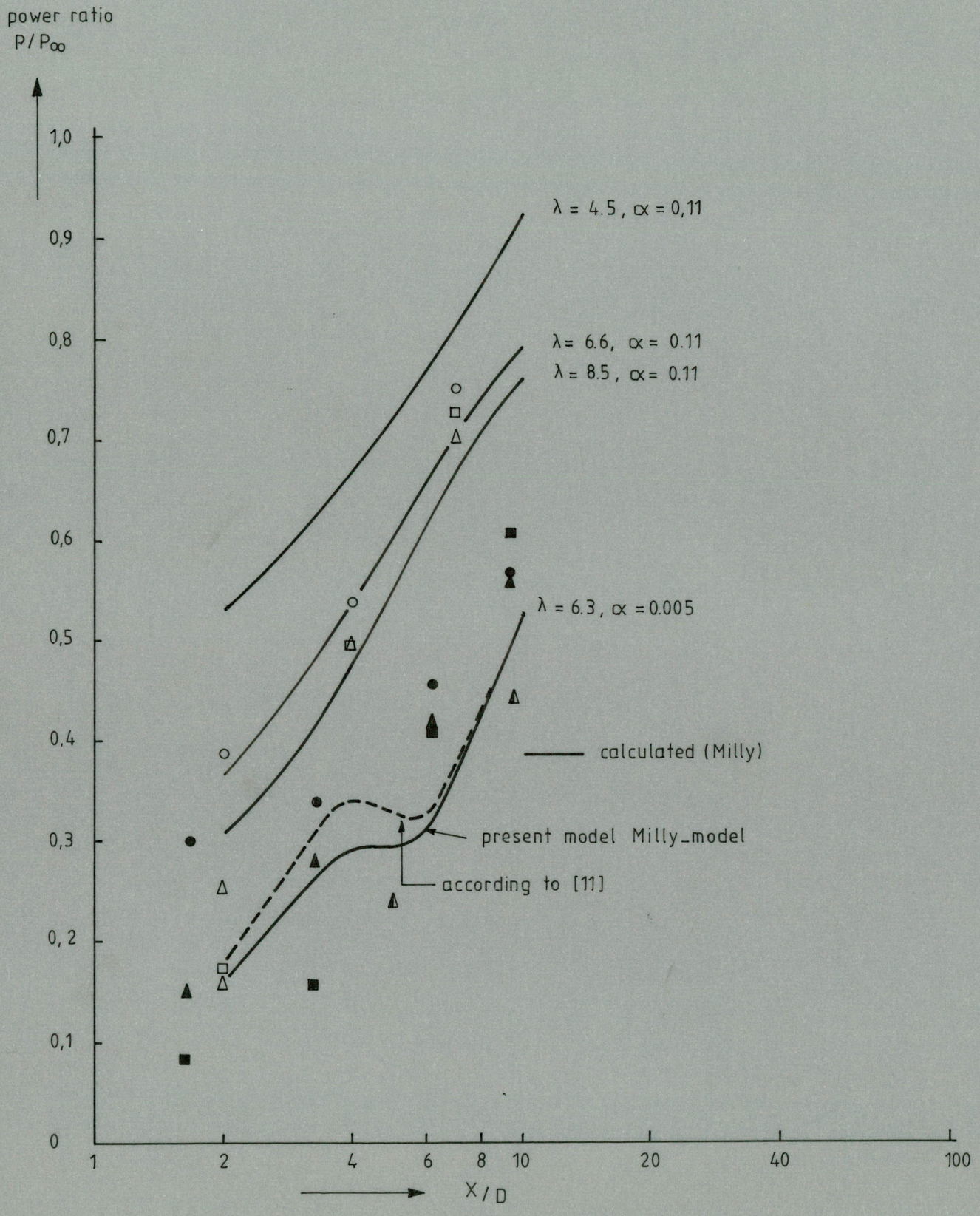

Calculated and measured power ratio as a function of the downstream distance

MT_TNO
12433
Fig. 17

Symbols : see fig.16

Calculated and measured power ratio as a function of the downstream distance

MT_TNO
1243
Fig.17

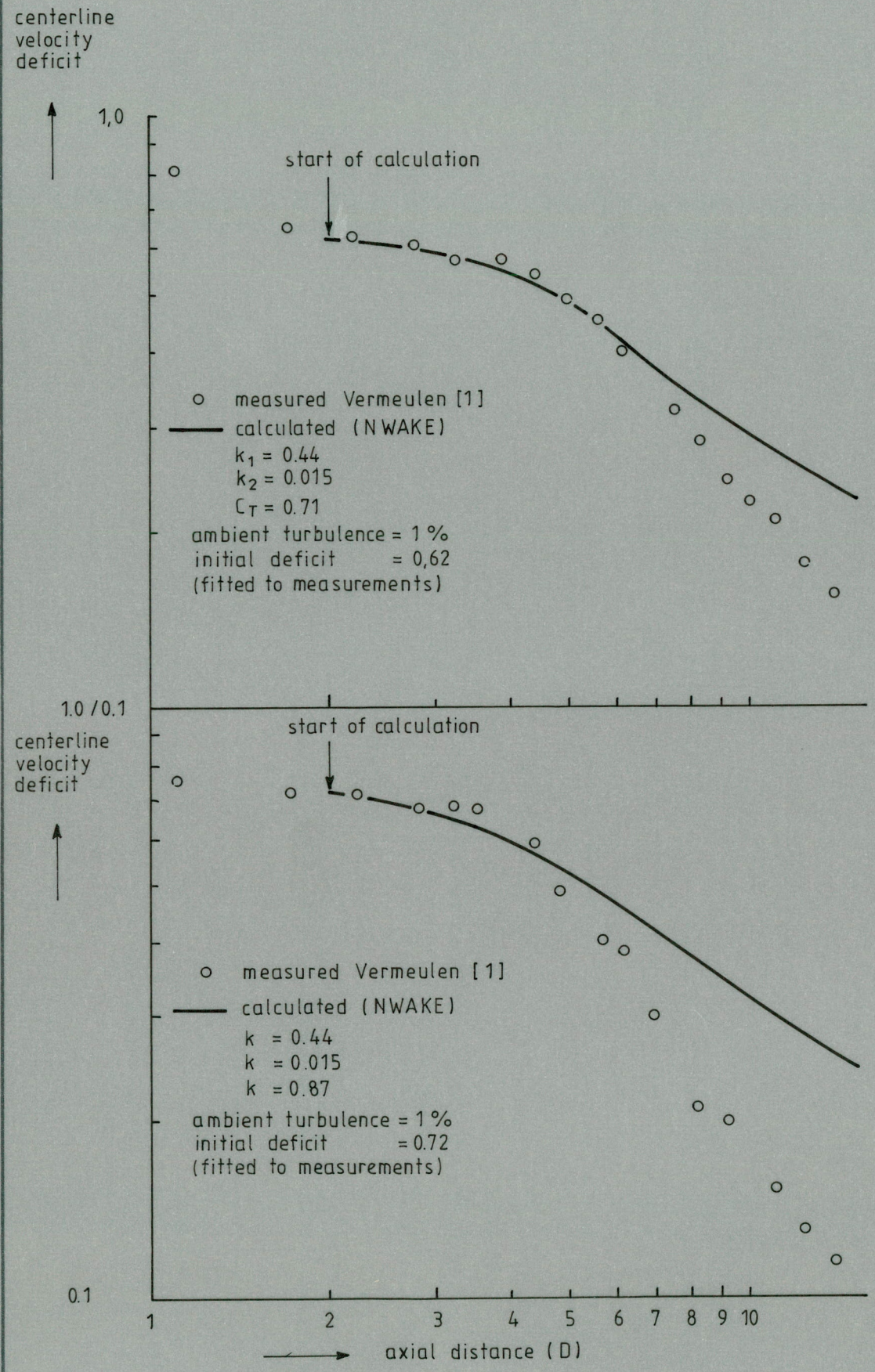

Measured and calculated centerline velocity deficit in uniform low turbulent flow

MT_TNO
12433
Fig. 18

Measured and calculated centerline velocity deficit in uniform low turbulent flow

MT_TNO
724 33
Fig. 18

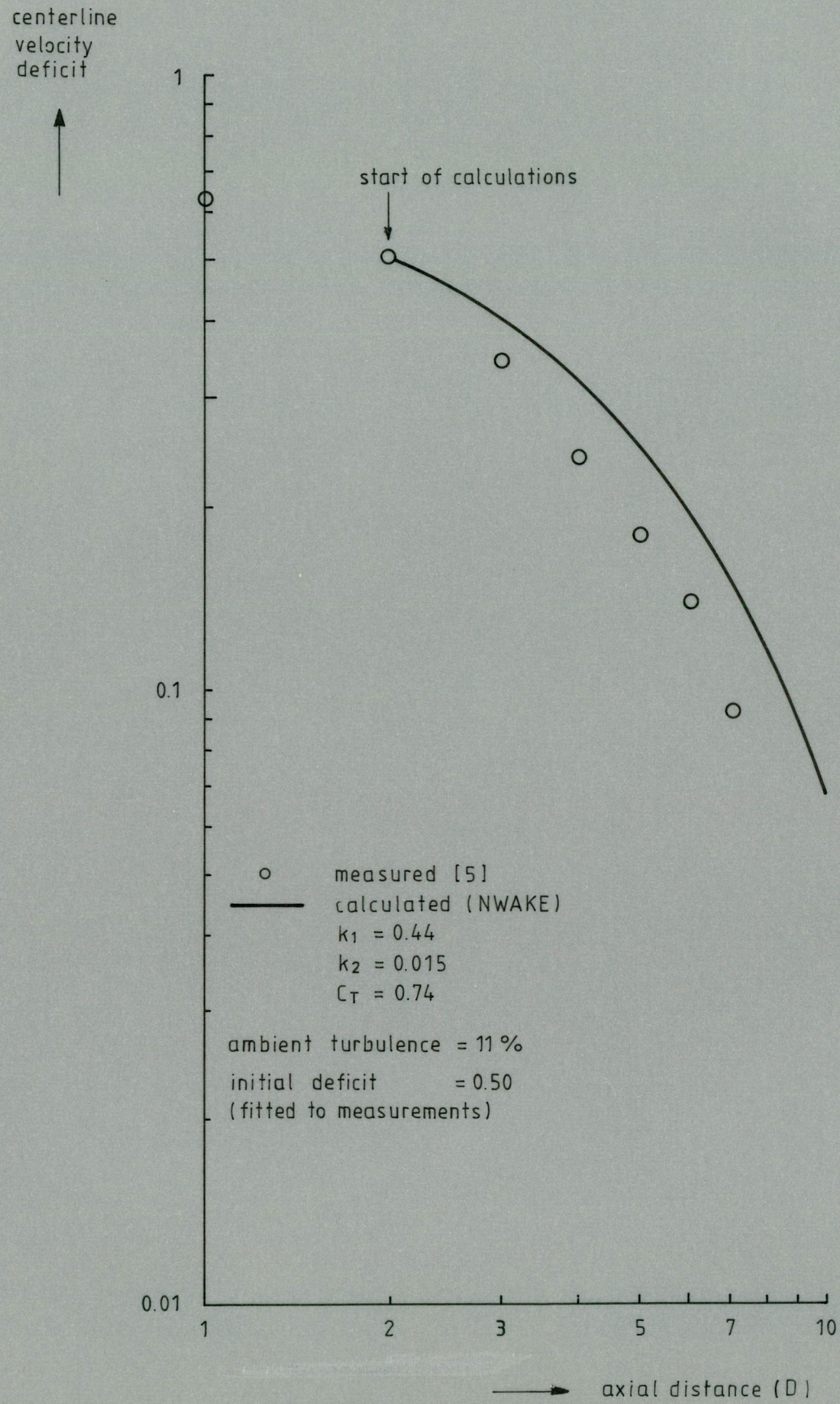

Measured and calculated centerline velocity deficit in simulated atmospheric boundary layer

MT_TNO
12433
Fig. 19

Measured and calculated centerline velocity deficit in simulated atmospheric boundary layer

MT_TNO
12433
Fig. 19

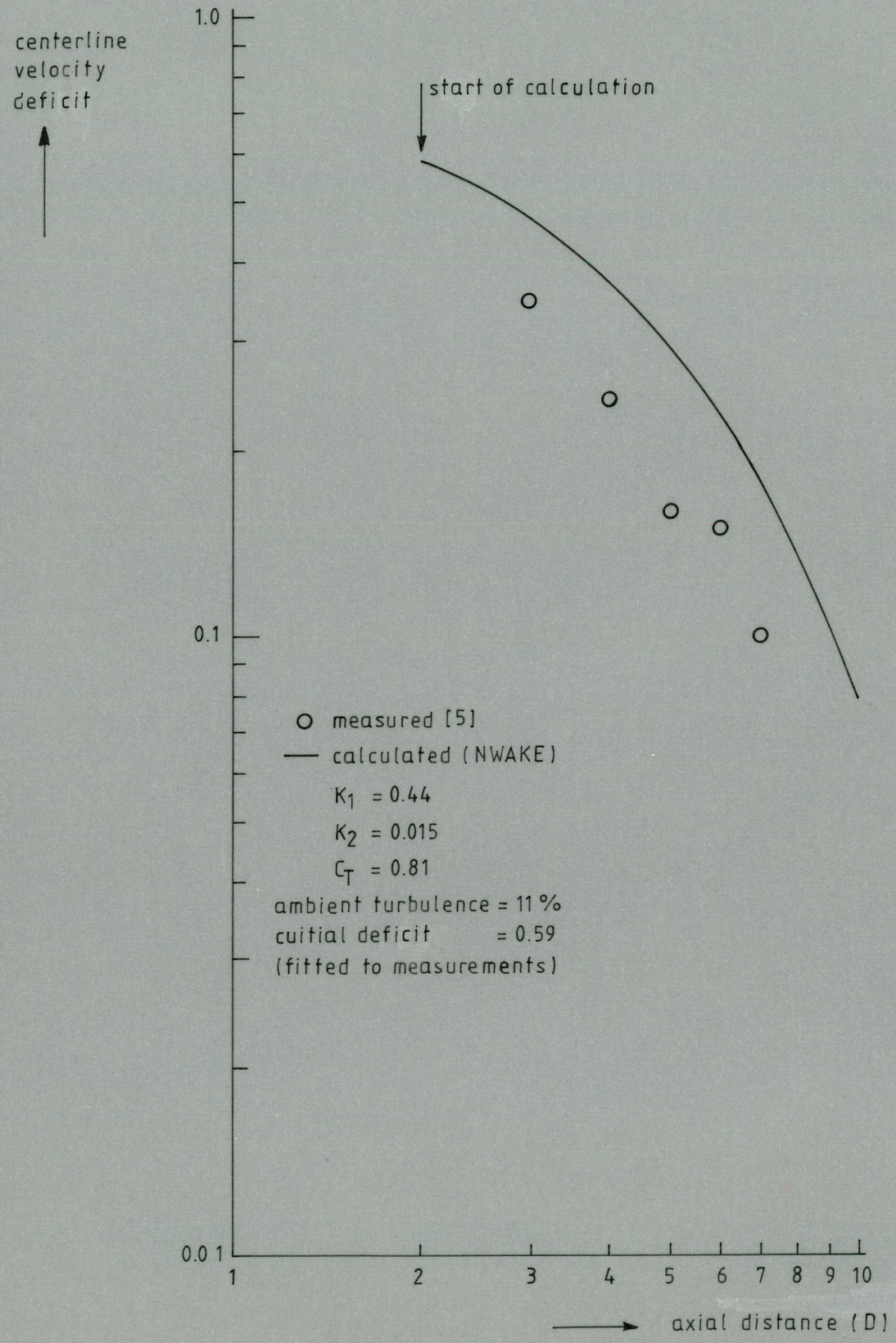

Measured and calculated centerline velocity deficit in simulated atmosferic boundary layer

MT — TNO
12433
Fig. 20

Measured and calculated centerline velocity defi
in simulated atmospheric boundary layer

MT — TNO
12433
Fig. 20

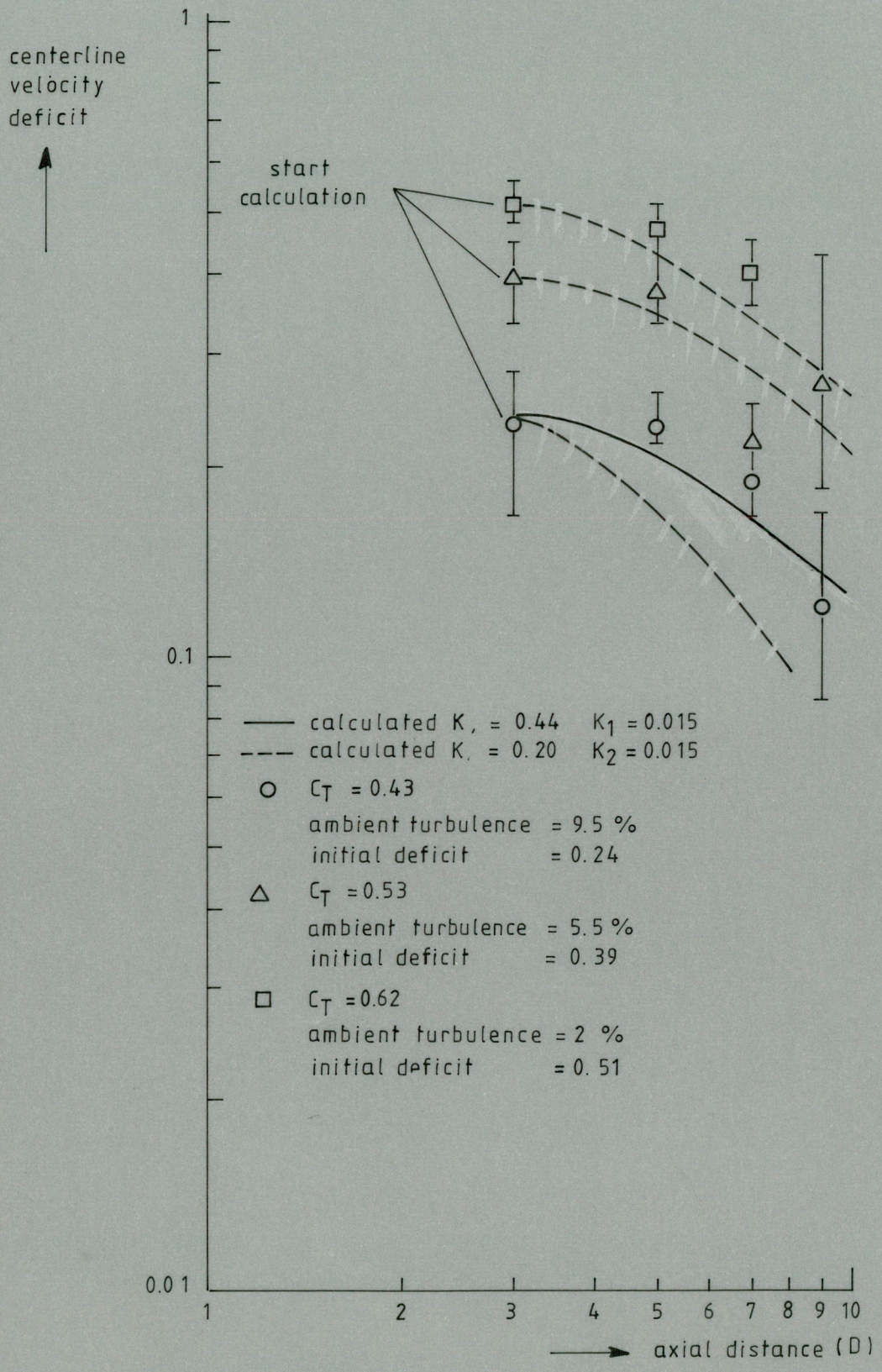

Comparison of NWAKE results with full scale data [8]

MT—TNO
12433
Fig. 21

Comparison of NWAKE results with full scale data [8]

MT—TNO
12433
Fig. 21

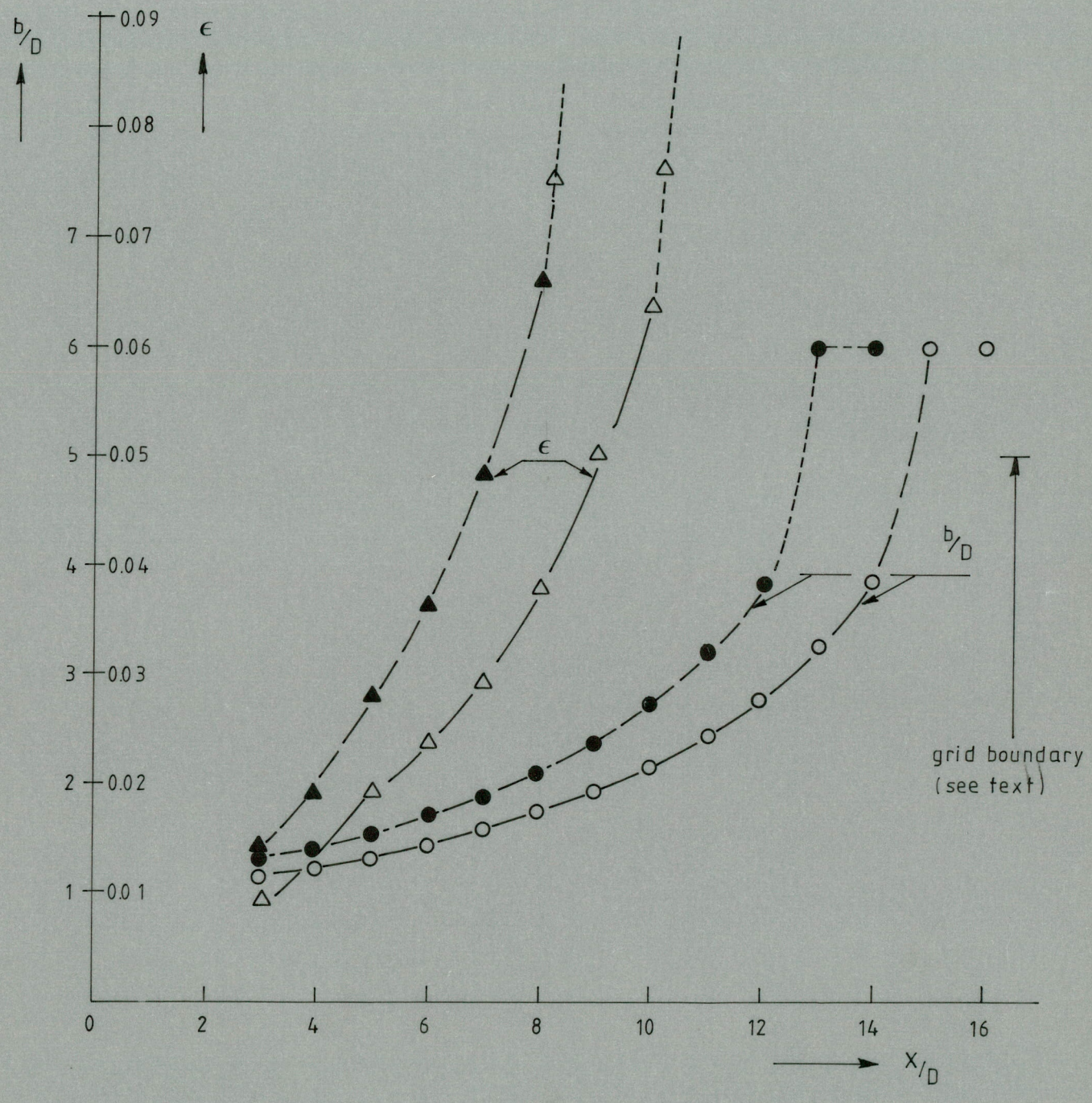

Calculated wake width (b/D) and eddy-viscosity (ϵ) in the NWAKE model

MT — TNO
12433
Fig. 22

Calculated wake width (b/D) and eddy-viscosity (ε)
in the NWAKE model

MT — TNO
1243 3
Fig. 22

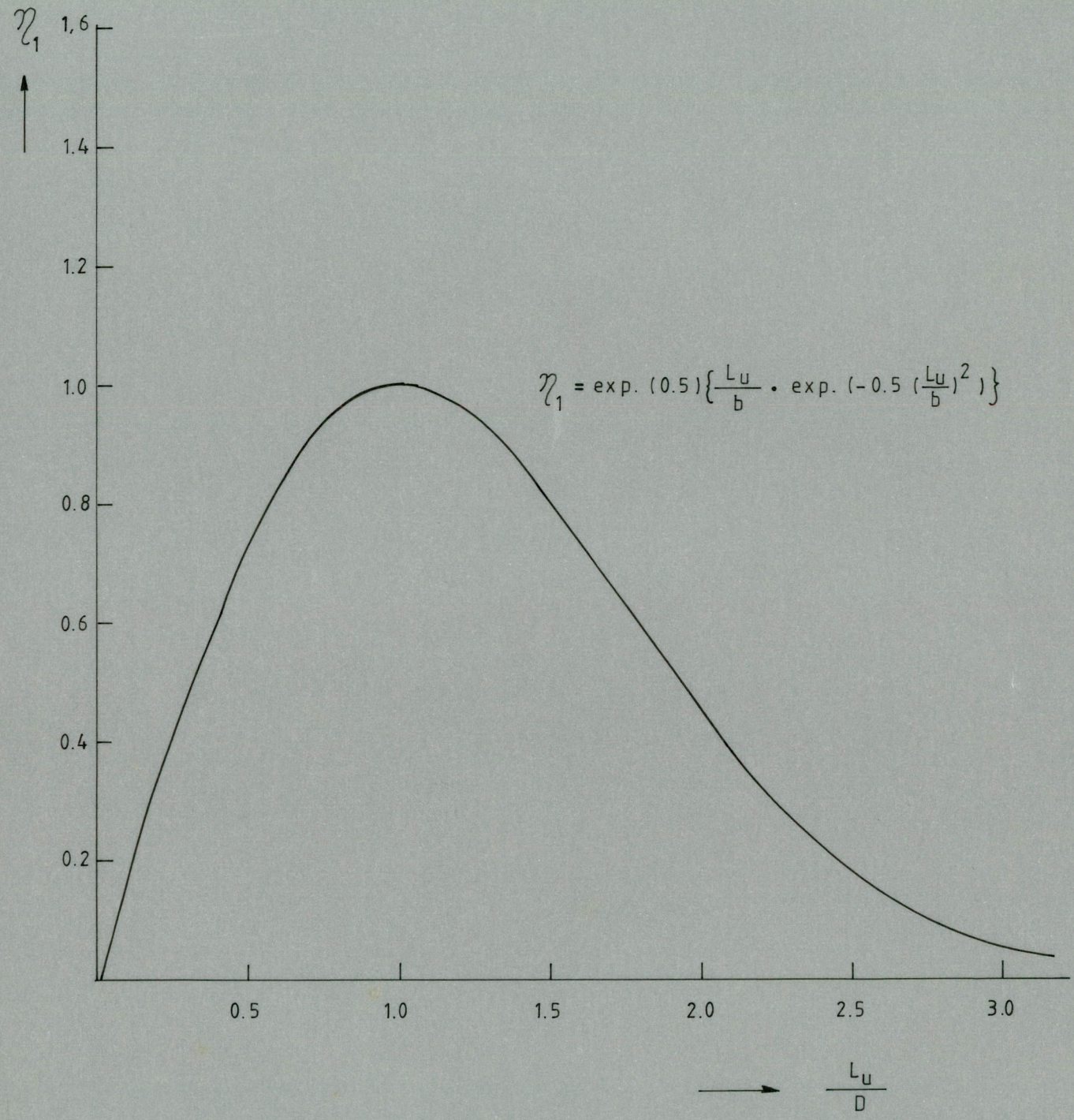

Estimated effect of ambient length scale wake diameter ratio on wake mixing efficiency

MT — TNO
12433
Fig. 23

Estimated effect of ambient length scale wake diameter ratio on wake mixing efficiency

MT — TNO
1243
Fig. 23

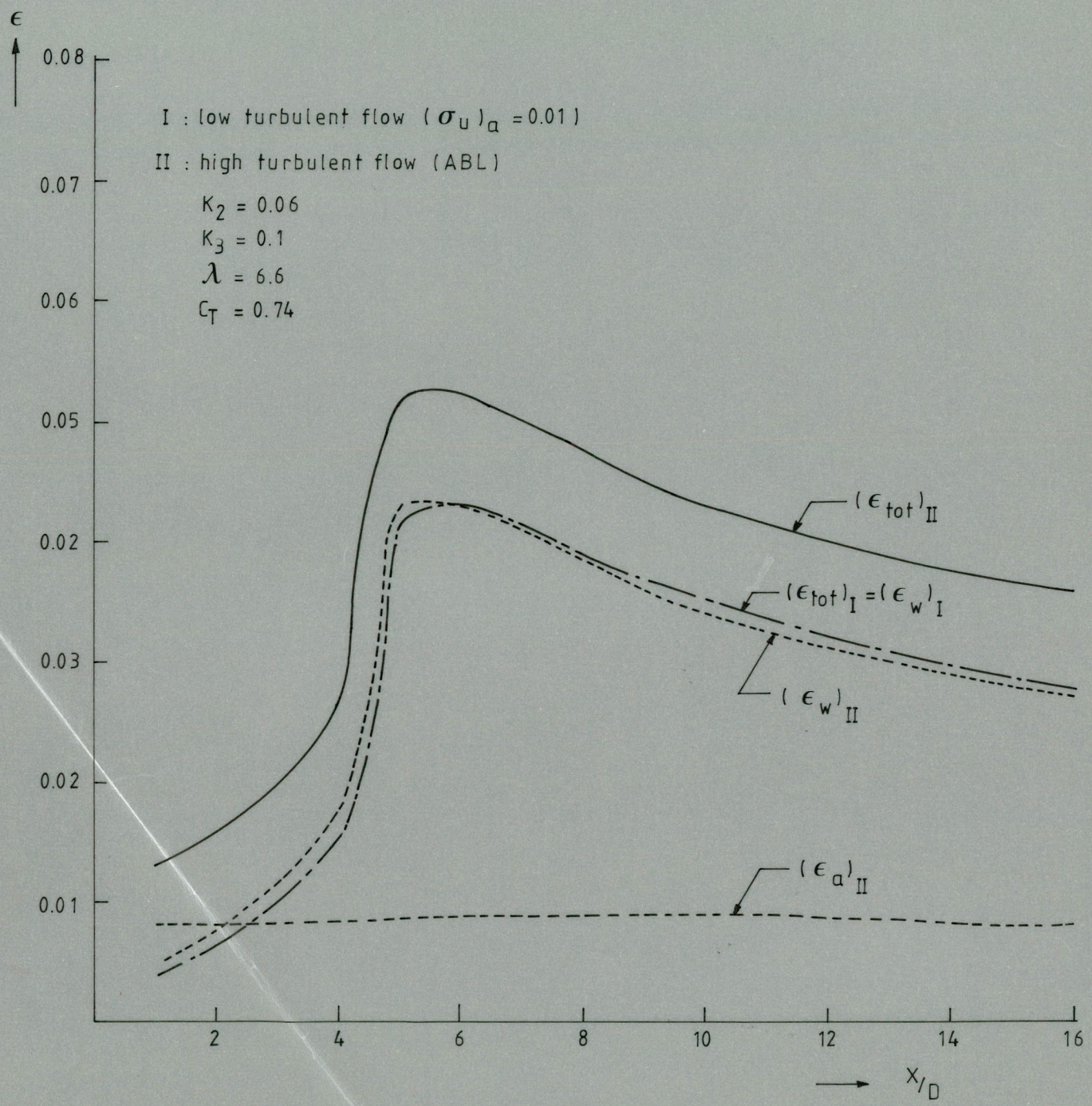

Effect of ambient turbulence on calculated eddy-viscosity	MT — TNO 12433 Fig. 27

Effect of ambient turbulence on calculated eddy-viscosity

MT — TNO
12433
Fig. 27

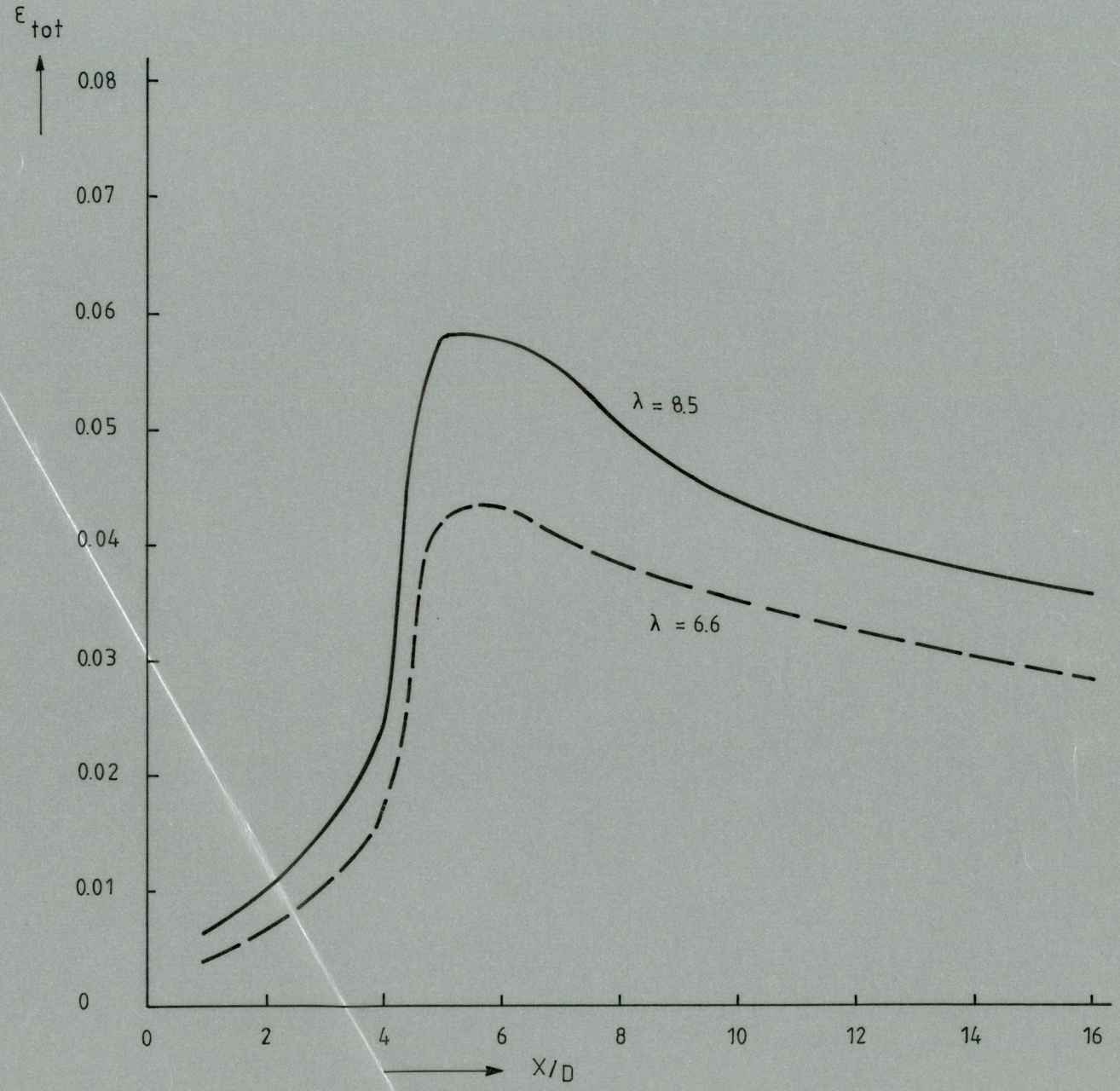

Effect of tipspeed ratio on calculated eddy_viscosity in low turbulent ambient flow ($\sigma_{u_a} = 0.01$)

MT_TNO
12433
Fig. 28

Effect of tipspeed ratio on calculated eddy_viscosity in low turbulent ambient flow ($C_{\mu a}$ = 0.01)

MT_TNO
12433
Fig.28